Faculdade de Engenharia da Universidade do Porto

U.PORTO
FEUP FACULDADE DE ENGENHARIA
UNIVERSIDADE DO PORTO

Nanoparticles as a Vehicle for a Novel Neuroprotective Drug to Fight Alzheimer's Disease

Mariangela Pasa

Dissertação realizada no âmbito do Mestrado em Engenharia Biomédica

Orientador: Dr. Joana Loureiro

Co-orientador: Dr. Maria João Ramalho, Prof. Maria José Diógenes

20th June 2023

Abstract

Alzheimer's disease (AD) is a neurodegenerative disease and the leading cause of dementia worldwide. To date, the therapies on the market for this disease are limited. This is due to, among many reasons, the difficulties in understanding completely the causes of the disease and the presence of the blood-brain barrier, a semipermeable border that prevents the entrance of solutes into the central nervous system. Therefore, the need to study new approaches for the targeted delivery of therapeutics to the brain.

In recent years, nanoparticles able to transport molecules across the blood-brain barrier have gained attention and are a promising approach for the targeted delivery of therapeutics to the brain. This project intended to develop nanoparticles to encapsulate compounds for AD therapy. The nanoparticles were characterized through their size, polydispersity index, zeta potential and encapsulation efficiency. Different types of nanoparticles produced by different methods were studied: poly(lactic-co-glycolic acid) (PLGA) nanoparticles - with a focus on both oral and nose-to-brain delivery – and solid lipid nanoparticles. PLGA nanoparticles produced by the double emulsion method showed to have good and stable size and zeta potential over the time of the study; however, the encapsulation efficacy of a hydrophilic test compound in these particles was low. With the protocol to produce PLGA nanoparticles through a single emulsion, it was possible to obtain nanoparticles with a mean diameter of 239.4 nm, a polydispersity index of 0.108 and a zeta-potential of -19.3 mV. A mean diameter close to 200 nm increases the chance for the particles to cross the blood-brain barrier, so even if the size is close to the goal, further optimization will be required. Other PLGA nanoparticles surface-modified with chitosan intended for nose-to-brain delivery were produced, having a mean diameter of 199.1 nm, a polydispersity index of 0.1075 and a zeta-potential of 6.3 mV, being suitable for the application. Lastly, the protocol to produce solid lipid nanoparticles was optimized, and it was possible to achieve particles with an average size of 236.6 nm, a polydispersity index of 0.277 and a zeta potential of -21.1 mV.

Acknowledgments

This thesis is the result of the candidate's work over a five-months period at the University of Porto thanks to the Erasmus+ program. The candidate worked under the supervision of Dr. Joana Loureiro, Dr. Maria João Ramalho and Prof. Maria José Diógenes at the Laboratory for Process Engineering, Environment, Biotechnology and Energy (LEPABE) of the Faculty of Engineering.

Contents

List of Figures

List of Tables

Acronyms, Abbreviations and Symbols

ACH   Amyloid cascade hypothesis

AChE Acetylcholinesterase enzyme

AD   Alzheimer's disease

AICD APP intracellular domain

BACE1 β-site APP-cleaving enzyme 1

BBB   Blood-brain barrier

CNS   Central nervous system

DE   Double emulsion

DLS   Dynamic light scattering

EDL   Electric double layer

EE   Encapsulation efficacy

EMA European medicines agency

FDA   Food and Drug Administration

NMDA N-methyl-D-aspartate

NP   Nanoparticle

PDI   Polydispersity index

PLGA Poly lactic-co-glycolic acid

PVA   Polyvinyl alcohol

rpm   Rotations per minute

SLNs Solid lipid nanoparticles

TC   Test compound

ZP   Zeta potential

Chapter 1

Introduction

1.1   Motivation

Alzheimer's is a type of dementia that affects memory, thinking and behavior. It is characterized by memory loss and cognitive impairment, loss of language and behavioral changes [1]. Although its cause is not entirely understood, the aggregation of amyloid beta peptides into fibrils that later leads to the formation of senile plaques is considered one of the key triggers of the disease. Thus, it is essential to find molecules able to prevent or interrupt fibrils' aggregation [2, 5].

Molecules, however, are not always able to cross the blood—brain barrier, a network of blood vessels and tissue that avoids that harmful substances can reach the brain. To overcome this problem, nanoparticles have gained a lot of attention in recent years [9, 33]. There are several nanoparticle types that differ in their physicochemical, biochemical and mechanical properties, presenting their own advantages and disadvantages [47].

The success of a neurodegenerative disease therapy depends not only on the pharmacokinetic and pharmacodynamic activity of the therapeutic agent. In fact, it depends to a large extent on its bioavailability and toxicity. It is, therefore, important to develop a nanocarrier with low toxicity that allows enhancing the therapeutic activity of promising therapeutic compounds [50].

1.2   Main objectives

The aim of the present work is to develop suitable nanoparticles as drug delivery systems for compounds to fight Alzheimer's disease. For this purpose, PLGA nanoparticles and solid lipid nanoparticles with controlled sizes and properties were prepared as nanocarriers. Their synthesis was complemented by physicochemical characterization of their structure and properties.

1.3   Thesis organization

This thesis is organized into five chapters. This chapter, "Introduction", presents a brief explanation of the motivation behind this research work as well as its main objectives. Chapter 2, "State of the art", presents theoretical knowledge and important concepts for the development and understanding of the work. In particular, it features an overview of Alzheimer's disease, the function and importance of the blood—brain barrier and currently available drugs. Lastly, drug delivery systems are explored, with a focus on PLGA nanoparticles and solid lipid nanoparticles. Chapter 3, "Nanocarriers for brain delivery", describes the methodology involved in the preparation and characterization of the PLGA nanoparticles and solid lipid nanoparticles. The materials employed during this work are presented as well. Chapter 4, "Results and discussion", summarizes the main findings of this research work. In Chapter 5, "Future perspectives", some concluding remarks and suggestions for possible future work to complement the present research are presented.

Chapter 2

State of the Art

2.1 Alzheimer's Disease

Most people's memory declines with age, so the line between normal age-related forgetfulness and the earliest signs of Alzheimer's disease (AD) can be very subtle. In fact, AD, which is the major cause of dementia, typically shows itself as a gradual loss of episodic memory (e.g. forgetting a conversation that took place the previous day) in an elderly individual. Progressively, other complications commonly emerge, such as difficulties with multitasking, recognizing people, and loss of confidence. As the condition advances, cognitive difficulties become more profound and widespread, interfering with activities of daily life [1].

At the microscopic level, AD is characterized by two neuropathological hallmarks: extracellular deposition of amyloid plaques and intracellular neurofibrillary tangles [2, 3, 4]. Several pathogenic mechanisms that underlie these changes have been studied, including amyloid β (Aβ) aggregation and deposition with plaques development, tau hyperphosphorylation with tangle formation, and other mechanisms such as inflammatory processes, oxidative stress, and mitochondrial dysfunction. The two most studied mechanisms are Aβ peptides aggregation and tau hyperphosphorylation. Although the cause of AD is not entirely understood, the aggregation of Aβ peptides into fibrils that deposit in senile plaques is considered one of the key triggers of the disease [5].

Before the early 2000s, the only sure way to know whether a person had AD was through autopsy. With the recognition that pathological changes occur years prior to symptoms and thanks to advances in research, imaging and laboratory tests are now available to help see biological signs of the disease in a living person [2]. The most common tests to diagnose AD are - besides an interview with symptoms review and a physical examination - blood tests and brain imaging. Tests are also performed to rule out other conditions which may cause, or more commonly contribute, to cognitive symptoms in the patients.

2.1.1 The Amyloid Cascade Hypothesis

The amyloid cascade hypothesis (ACH) for AD has been very influential in research since it was posited in 1992 by Hardy and Higgins [5, 6]. According to the original ACH, the accumulation of Aβ peptides in the brain parenchyma and the consequent aggregation and deposition in the form of amyloid plaques is the central event in the pathogenesis of Alzheimer's pathology. As knowledge of pathological changes in AD increased, research focused on more specific alterations in Aβ processing, namely the cleavage of the amyloid protein precursor (APP) into the Aβ_{1-40} and Aβ_{1-42} peptides, and on the importance of Aβ oligomers (i.e., small aggregates of 2 to 12 peptides) [6, 7].

Aβ peptide is a normal metabolic product that can be found in the cerebrospinal fluid of healthy individuals. It is released from APP – a transmembrane protein that has the general properties of a cell surface receptor - after the sequential cleavage by two enzymes. APP can be processed through two main pathways: the non-amyloidogenic and the amyloidogenic pathway. In the non-amyloidogenic pathway, APP is cleaved by the enzymes α-secretase and γ-secretase. The cleavage of APP by α-secretase generates two fragments: the amino-terminal fragment sAPPα and the carboxy-terminal fragment CTF83. The following cleavage of CTF83 made by γ-secretase will result in the generation of p3 – a soluble peptide without a tendency to aggregate - and the amino-terminal APP intracellular domain (AICD). Otherwise, if APP is subsequently cleaved by β-secretase and γ-secretase, the neurotoxic Aβ peptide is biosynthesized. In this case - the amyloidogenic pathway - the cleave by β-secretase generates the amino-terminal fragment sAPPβ and the carboxy-terminal fragment CTF99. The following γ-Secretase cleavage of CTF99 will result in the generation of Aβ and the amino-terminal APP intracellular domain (AICD). When the neurotoxic Aβ peptide's concentration increases by overproduction or defective clearance, Aβ self-aggregates into assemblies ranging from oligomers to insoluble fibrils and, lastly, to amyloid plaques. In particular, amyloid plaques are extracellular accumulations mainly composed of abnormally folded Aβ peptides with 40 ($\sim$90%) or 42 ($\sim$10%) amino acids, respectively Aβ_{1-40} and Aβ_{1-42}. The Aβ_{1-42} peptide aggregates more readily than Aβ_{1-40} and the ratio of these two isoforms is influenced by the pattern of cleavage from APP by α-, β- and γ- secretases [6, 22]. The amyloid deposition does not always follow a characteristic pattern of progression but, broadly speaking, develops in the isocortex and only latterly affects subcortical structures. The Aβ deposition and diffused plaque formation lead to local microglial activation, cytokine release, reactive astrocytosis and a multi-protein inflammatory response.

The amyloid cascade hypothesis also proposes that changes in tau, a microtubule-associated protein, and the consequent neurofibrillary tangle formation are triggered by toxic concentrations of Aβ. Tau is a soluble protein, but insoluble aggregates are produced during the formation of neurofibrillary tangles, which disrupt the structure and function of the neuron. Tau monomers first bind together to form oligomers, which then aggregate
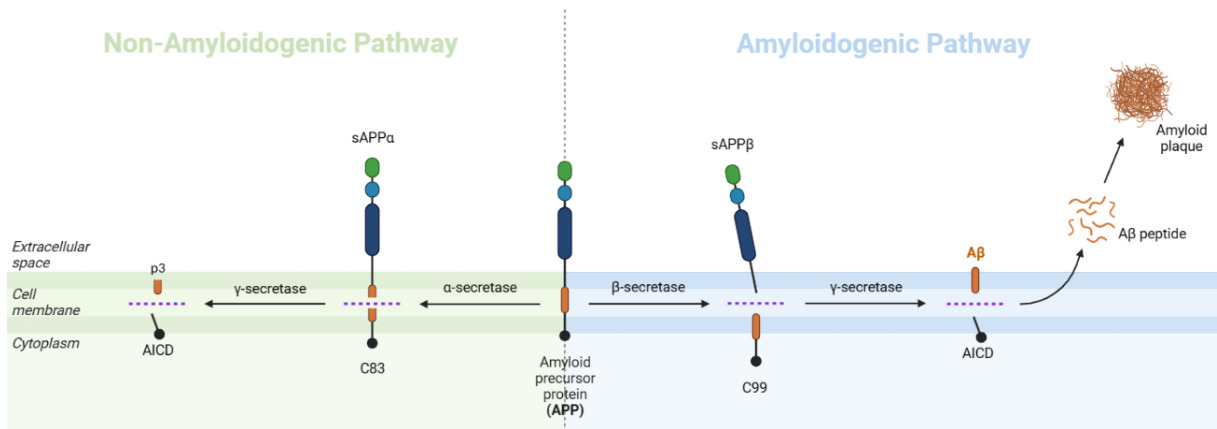
Figure 2.1: Schematic representation of non-amyloidogenic and amyloidogenic pathways

into a β sheet before forming neurofibrillary tangles [6, 8].

2.2 Treatment Strategies for Alzheimer's Disease

Therapeutic approaches to AD can be divided into three categories: symptomatic, disease-modifying and regenerative [10].

Most of the existing treatments are symptomatic and aimed at ameliorating cognitive function. However, they only contribute to modest benefits in symptom management. In addition, they do not prevent neuronal loss, brain atrophy and, consequently, the progressive deterioration of cognition [4, 10, 11]. Most ongoing efforts are to find new therapies focusing on modifying the progression of AD [11]. The idea behind these disease-modifying drugs is to delay the onset or change the course of the disease, so people will live longer and without developing AD. To date, approaches have largely focused around intervention in the $A\beta$ cascade and tau biology [12, 13, 14]. The third category, regeneration, remains a very hypothetical approach. Indeed, regenerating a diseased brain or replacing lost neurons is arguably a step too far for AD at present [10, 11].

In the decade from 2002 to 2012, drug development for AD has proven to be extremely difficult, with a 99.6% failure rate; currently, the success rate continues at the same level [15]. Each trial is a test of a narrow hypothesis that incorporates decisions that offer insights into the AD drug development, such as the dosage to be used, the target population and the exposure duration [16]. In addition, it is important to learn lessons from other trials in order to improve the likelihood of success. For example, since the beginning of the studies, the maximum tolerated dosage of the drug should be determined, as well as if it can cross the blood-brain barrier. Moreover, since AD biology is complex and not completely known, the use of a single key biomarker should be avoided, while multiple biomarker outcomes should be collected [15, 16].

2.2.1 Symptomatic Drugs: Current Commercial Drugs

At present, most of commercial drugs are symptomatic drugs. This means that existing commercial treatments can improve symptoms or delay the decline of the disease but cannot impact the disease's underlying neurodegenerative process [10, 17]. Four therapies are currently approved by the Food and Drug Administration (FDA) for AD and have two different modes of action: agonism of the cholinergic system and antagonism of the N-methyl-D-aspartate receptor (NMDA). Donepezil, galantamine and rivastigmine are inhibitors of the acetylcholinesterase enzyme (AChE); memantine opposes glutamate activity by blocking NMDA receptors. Another AChE inhibitor, tacrine, had been approved by the FDA but was withdrawn from the market in 2013 due to its association with significant liver toxicity [14].

It has been postulated that the loss of cholinergic neurons and the consequent impairment in dopaminergic transmission could be the main factors underlying AD-related psychiatric symptoms [18, 19]. Acetylcholine is a neurotransmitter that is released into the synaptic space by the presynaptic neuron and binds to receptors in the postsynaptic neuron. This molecule is subject to enzymatic degradation by one of the several cholinesterases, the AChE citetreatment. Although there are some differences in putative mechanisms, donepezil, galantamine, and rivastigmine bind to AChE, reducing the normal enzymatic degradation of acetylcholine and thus increasing the bioavailability of acetylcholine at the synapse. In this way, neurotransmission is enhanced by preventing acetylcholine's hydrolysis and, subsequently, increasing its synaptic levels [11, 17].

While AChE inhibitors were used in clinical practice for mild to moderate AD, there
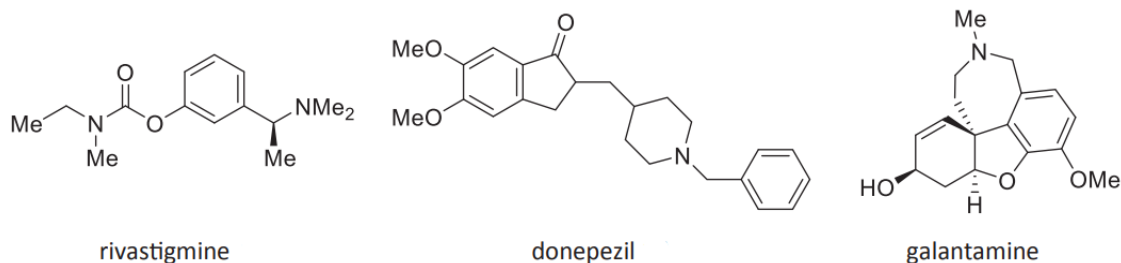
Figure 2.2: FDA-approved acetylcholinesterase enzyme (AChE) inhibitors

were no available treatments for patients with moderate to severe AD until 2003, when FDA approved memantine. Memantine is the sole NMDA antagonist medication available for AD approved by the FDA [10]. It targets glutamatergic dysfunction and exhibits its mode-of-action by binding to the open state of the NMDA receptor channel. Its precise mechanism of action is uncertain, but it is thought to reduce the excitatory neurotoxicity effect of glutamate [11, 10, 12]. One hypothesis as to how memantine works is by normalizing the increased activity of NMDA receptors that has been reported in several neurodegenerative diseases, including AD. The normal function of the NMDA receptor

allows Ca^{2+} influx for neurotransmission; however, in disease situations, an increased activity of the NMDA-receptor may cause prolonged channel opening, leading to excessive Ca^{2+} influx, which then triggers downstream events that ultimately lead to neurodegeneration [12].

2.2.2 Disease-Modifying Strategies: Targeting Amyloid β and Tau

Symptomatic drugs do not stop or delay the progression of the disease by affecting the underlying pathogenic mechanisms, but only provide short-term benefits [20]. The development of disease-modifying treatments, able to counteract the progression of AD, is thus a big challenge. Many disease-modifying treatments candidates for AD have been proposed, but to date, only two have been approved by the FDA. All the others have not been approved due to failure during clinical trials [20, 21].

Drugs can fail due to different reasons. Since the pathophysiological process of AD begins years before its diagnosis, the optimal time for disease-modifying treatment may be in the pre-symptomatic stage of AD, where the disease is still hidden. Therefore, initiation of the treatment when AD is already developing might not be appropriate [22]. Other reasons for drugs to fail are the inappropriate drug dosage or their inability to cross the blood-brain barrier and, therefore, reach the brain.

Disease-modifying treatments can be divided in different categories with respect to their targets.

Active and passive immunization

Immunotherapies are under investigation for AD. While both active and passive immunotherapies strive to slow or prevent the cognitive decline linked with AD, each has its own advantages and disadvantages.

The concept of immunotherapy for neurodegenerative diseases was introduced by Schenk in the 90s when he tried to use an $A\beta$ vaccine to tackle AD [20, 23]. Following the failure of the first vaccine in the early 2000s, Bard and colleagues demonstrated that the transfer of anti-$A\beta$ antibodies eliminated $A\beta$ in the brains of APP-transgenic mice. Some clinical trials are being carried out and, in patients with early AD, the administration of anti-amyloid antibodies has shown to reduce plaque volume, suggesting that passive immunotherapies may be promising [24, 25].

Aducanumab was the first monoclonal antibody that targets $A\beta$ aggregates approved by the FDA in 2021 for the treatment of mild AD. This antibody removes amyloid plaques and, when used at higher doses, has shown to have a modest impact on the cognitive decline of patients at the early stage of AD [26, 27]. However, there is a lack of correlation between the reduction of $A\beta$ plaques and clinical improvements in trials to date. In addition, there are also considerable concerns about the safety of this new drug. Indeed,

patients treated with aducanumab had a higher incidence of brain swelling and intracerebral hemorrhages. For these reasons and the divergent outcomes of clinical trials, the European Medicines Agency (EMA) rejected the marketing authorization for aducanumab [27, 28].

Lecanemab was approved in January 2023 by the FDA, becoming the second disease-modifying treatment approved for AD in the USA. According to the prescribing information, the treatment should be initiated in patients with mild cognitive impairment or mild dementia with a confirmed presence of Aβ [29]. Lecanemab is a monoclonal antibody directed against aggregated soluble and insoluble forms of Aβ peptide. In clinical trials, lecanemab has been shown to clear amyloid from the brain successfully. However, clearance had no discernible effect on cognition in some trials, a very small and non-significant effect in other trials, and a very small significant effect in the latest trial. In addition, lecanemab comes with safety concerns. Indeed, during the trials, some participants developed brain oedema, experienced brain haemorrhage and/or other adverse events severe enough to discontinue the trial [29, 30]. Lecanemab is now undergoing regulatory review in the European Union, Japan and China.

β-secretase and γ-secretase inhibitors

Inhibitors of APP-cleaving enzymes have been anticipated as potential drugs for AD.

γ-secretase is a protease complex that cleaves proteins. The most known substrate of γ-secretase is APP, whose cleavage Aβ. Its inhibition aims to decrease the production of Aβ, including the toxic Aβ_{40} and Aβ_{42} [20, 21, 23]. Among all the γ-secretase inhibitors, three reached phase 3 studies before being abandoned. This is because they were associated with a worsening of daily function, increased rates of skin cancer and infection and/or low brain penetration. In addition, the development of γ-secretase inhibitors presents problems related to their potential nonspecific effects since γ-secretase is involved in the cleavage of several proteins [22, 23].

The development of β-site APP-cleaving enzyme 1 (BACE1) inhibitors took much longer than γ-secretase inhibitors took. BACE1 accounts for most of the β-secretase activity in the central nervous system, thus, its inhibition is expected to reduce the total production of Aβ [20, 21]. Many BACE1 inhibitors failed due to a lack of efficacy. These drugs were demonstrated to lower Aβ_{40} and Aβ_{42}, but failed to prove clinical benefit, and in some cases, adverse effects were observed. Moreover, because BACE1 also has other substrates, the development of inhibitors might face problems of toxicity related to non-specific effects [22, 20, 23].

Anti Tau strategies

The other pathological hallmark of AD, neurofibrillary tangles, consists of intracellular aggregates whose main constituent is a hyperphosphorylated form of the protein Tau

[20, 21]. Tau has received less focus as a therapeutic target, and the strategies that have been used to target it concern the development of inhibitors of Tau-phosphorylation and compounds that prevent Tau aggregation and/or promote disassembly [21, 23].

2.3   The Blood-Brain Barrier

The central nervous system of adults lacks a significant capacity for regeneration. The cerebral microenvironment is therefore maintained by the tight regulation of molecular traffic and is the result of specific anatomical and biochemical properties of the various interfaces [31].

2.3.1   The blood-brain barrier structure

Unlike peripheral capillaries that allow relatively free exchange of substance across cells, the blood-brain barrier (BBB) rigorously limits transport into the brain. The BBB functions as a physical barrier and also as a biochemical barrier that expresses certain enzymes to protect any actions towards the brain environment. Thus, the BBB is often the rate-limiting factor in determining the permeation of therapeutic drugs into the brain.

In our body, numerous biological barriers separate the circulating blood from the interstitial fluid that surrounds tissues [32]. The BBB is the interface between the vascular system and the brain and is perhaps the most selective of these barriers, reflecting the brain's crucial role. The brain does not have an outstanding ability to store metabolic nutrients, so oxygen and glucose are provided by the vascular system [33]. Therefore, the barrier function of the BBB is essential for regulating transport to the brain of nutrients, but also represents a significant roadblock for the invasion of toxins and pathogens and for the delivery of drugs to the brain.

To sustain this robust barrier, the endothelial cells of central nervous system (CNS) have distinct properties from the endothelial cells in other tissues [32]: BBB-specific transporter and receptor proteins control entry and exit of metabolites across cells (transcellular transport); high electrical resistance tight junctions significantly reduce the permeation of ions and polar solutes through paracellular transport and effectively block penetration of macromolecules [33, 34]; few transcytotic vesicles and absence of fenestrae avoid the passage of molecules in peripheral endothelial cells.

For these reasons, the BBB is the most important factor limiting the development of therapies for the CNS, including neurodegenerative diseases, such as AD. Indeed, the BBB limits the brain penetration of most CNS drug candidates. Therefore, methods to study the transport of drugs and other molecules across the BBB are key to understanding how the BBB regulates the transport of molecules and will be invaluable for drug discovery and treatment of CNS diseases.

2.3.2 Strategies to cross the blood-brain barrier

At the BBB, various means of transport are employed for physiological cargoes that could also be utilized for drug delivery. Due to the presence of tight junctions, few molecules can diffuse across two adjacent BBB endothelial cells. Therefore, molecules with a molecular weight lower than 500 Da might passively diffuse through the membranes of the endothelial cells of the BBB following their concentration gradients [35, 36]. This is the case of gasses such as, for example, oxygen and carbon dioxide. In addition, lipid-soluble molecules can enter the brain by diffusion depending on their lipid solubility and molecular weight [35]. However, these properties are not an absolute indication of CNS penetration. For the largest molecules, the transcellular route across the BBB endothelial cells requires their interaction with specific receptors. This process is highly specific and, to date, remains poorly understood.

Delivery of therapeutic molecules modifying their physicochemical properties

The transport across the BBB of small molecular drugs mainly occurs by passive diffusion. The "Rule of 5" is an empirical approach to predict if a molecule will diffuse through the BBB, that was proposed by Lipinski in 2001. This precept states that molecules with a molecular mass lower than 500 Da, no more than 5 hydrogen bond donors, no more than 10 hydrogen bond acceptors and a LogP value not higher than 5 have a higher chance to passively diffuse across the BBB. Thus, these four parameters must be optimized to improve the BBB permeability of therapeutic molecules by passive diffusion [31, 35].

Modulation of the blood-brain barrier permeability

Considering that the BBB is the major obstacle to an efficient CNS delivery of therapeutics, another strategy involves the opening of this barrier. In contemplating this option, it needs to be ensured that the BBB is only opened transiently and selectively. In addition, the opening of the barrier must take place in a controlled and reproducible manner, with no short- or long-term adverse effects [31].

Originally, the use of hyperosmotic agents to achieve reversible BBB opening was commonly used. However, the BBB opening caused by these agents is non-selective and also differs for various brain regions. This could cause an uncontrolled influx of low and high molecular weight compounds in the brain, leading to neurological toxicity. Another strategy that has been pursued is the modulation of tight junctions. For this purpose, protein-binding agents and chemicals have been applied. However, for the clinical translation of this modality, more mechanistic studies are required [31].

Nanoparticles to cross the blood-brain barrier

Since the early 1990s, nanoparticles have been used to improve drug delivery to the brain and have immediately shown promising results. Nanoparticles are not only able to protect their cargo from rapid degradation and clearance, but they can also be functionalized or modified to cross the BBB more easily. Indeed, nanoparticles' delivery will depend on several factors, including their size, coating, surface charge and functionalization [35].

However, it is not yet possible to identify ideal parameters for these factors. For example, conflicting results have been obtained for the nanoparticle's charge. For instance, examples of nanoparticles with positive, neutral and negative zeta potentials have been reported to efficiently cross the BBB [35].

2.3.3   Delivery of Actives through the Blood-Brain Barrier

The route of drug administration is defined as the path by which a drug is taken into the body and plays a marked role in the bioavailability of the actives in the body. For a drug to produce its desired therapeutic effect, it must come in contact with the targeted regions of the body, and for this to happen, the drug must be administered in the appropriate manner. The routes of administrations are classified into local and systemic. The local
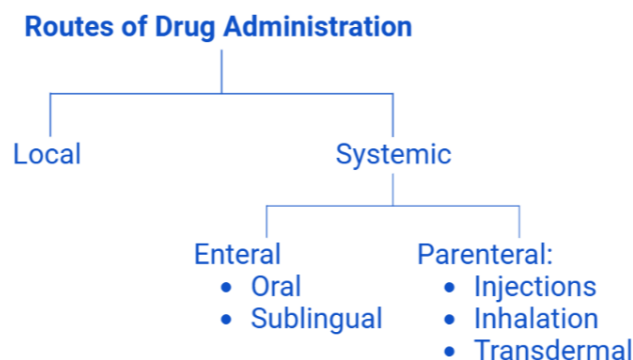
Figure 2.3: Routes of drug administration

route is the simplest mode of administration of a drug. In this case, the drugs are directly applied to the skin or the mucous membrane to achieve a local action. On the other hand, the systemic administration of drugs involves the passing of the substances into the circulatory system, so that the entire body is affected. When the systemic absorption of a drug is required, medications can be administered by two main routes: the enteral and the parenteral route. Enteral administration involves the absorption of the drug through the gastrointestinal tract. Methods of administration include the oral, sublingual and rectal administration. On the other side, a parenteral route is any route that is not enteral and, thus, does not involve drug absorption via the gastrointestinal tract. Parenteral

11

administrations include injections (e.g., intravenous, intramuscular and subcutaneous), inhalations and transdermal routes [37, 38].

The reason for choosing a route of drug administration rather than another is governed by many factors, which include:

- Physico-chemical properties of the drug and the effect of gastric pH, digestive enzymes and first-pass metabolism on the drug. Indeed, some drugs may be effective only if administered by one specific route

- Whether the agent is being administered for a local or a systemic effect

- Convenience. Enteral routes are generally the most convenient for the patient, as no punctures or sterile procedures are necessary. For this reason, they are often preferred in the treatment of chronic disease

- Condition of the patient.

Below, the oral delivery system and the intranasal route are analyzed.

Oral Administration

The oral delivery is the most widely used since it offers many advantages. It is non-invasive and usually meets patients' compliance. Moreover, oral formulations are less expensive to produce compared to others and are amendable to self-administration. However, it is not always feasible for the delivery of certain drugs due to their instability in the gastrointestinal tract [39, 40]. That is why oral delivery can benefit from the use of nanoparticles. Nanoparticles can help overcome many of the barriers encountered following oral administration, enzymatic degradation and poor membrane permeability. Three different scenarios can occur for nanocarriers at the gut level [38, 40]:

1. They may be absorbed intact along with the cargo into the systemic circulation

2. They can fuse or interact with the intestinal membrane, aiding the absorption of the cargo but without absorbed

3. They might prematurely release the cargo in the gut lumen prior to interacting with the intestinal membrane, leading to a possible degradation of the compound

Due to these challenges, other administration routes are often considered.

The Intranasal Route: Nose-to-Brain Delivery

The nasal route has been suggested as an alternative to the parenteral and oral routes. Drug administration through the nasal route is possible since the tightness of the intercellular junctional complex of the nasal mucosa is low, making it relatively permeable, and the mucosa is extensively vascularized, enabling a rapid and optimal absorption of drugs to the bloodstream [41, 42].

More recently, the nasal route has been studied for the direct brain delivery of drugs. This way of administration represents a promising alternative to other delivery systems since it allows active pharmaceutical ingredients to be directly delivered into the brain and has several benefits over traditional drug administration systems. It allows to bypass of the BBB, prevents drug degradation in the gastrointestinal tract, and avoids the first-pass metabolism that occurs in the liver. In addition, it increases the bioavailability of low molecular weight agents, and it is a convenient non-invasive administration route [41, 43]. However, some anatomical and physiological features – such as the high enzymatic activity in the mucus layer and the mucociliary clearance process of the nose cavity, that restrict intranasal absorption - might present a limitation for this type of delivery. To overcome these drawbacks, the use of nanoparticles for intranasal drug delivery has been implemented. Numerous mucoadhesive polymers are used to prolong the period of adherence in the nasal cavity, such as chitosan, alginate and cellulose. Furthermore, the use of positively charged nanoparticles proved interesting results since they interact with the anionic mucin of the nasal cavity [44].

2.4 Nanotechnology for Brain Delivery

The production and formulation of drugs play a crucial role in their effects. Indeed, the therapeutic activity of a drug can be compromised by factors such as pH and temperature and, in the case of peptides, is highly dependent on their flexible conformational structure [45]. Therefore, drug delivery is one of the main challenges regarding the stability of the drug itself. "Drug delivery" describes the technologies that carry drugs into or throughout the body. These technologies include the method of delivery, such as injection or ingestion, but also describe the way that drugs are 'packaged' - like liposomes or nanoparticles – to protect them from degradation. Indeed, to enhance their therapeutic effects and reduce the related side effects, active drug molecules should selectively accumulate in the disease area and not deteriorate before arriving in their targeted zone.

From the last few decades nanoparticles have attracted considerable interest in targeting drug molecules to the brain, since nano-delivery systems have great potential to facilitate the movement of drugs across barriers (e.g., the BBB). A nanoparticle (NP) is defined as a nano-object with all its three dimensions ranging from approximately 1 nm to 1000 nm [46, 47]. A common misconception is that small molecules readily cross the

BBB. In fact, more than 98% of all small molecules do not cross the BBB either [48]. For a small-molecule to cross the BBB, two molecular characteristics are required: high lipid solubility and low molecular mass (i.e., the molecular mass has to be lower than 400–500 Da). However, only a few diseases of the brain, such as depression, chronic pain and epilepsy, consistently respond to this category of small molecules. Unfortunately, many other disorders including AD, do not have a neurotherapy that can stop the neurodegeneration [49].

Several nanoparticles have been developed to transport and protect the desired molecules in the brain. One of the key characteristics of nanoparticles is their size. It is known that spherical particles bigger than 200 nm are efficiently filtered by liver, spleen and bone marrow, while particles smaller than 10 nm can be quickly cleared by the kidney or through extravasation. Thus, the ideal size range for the circulating carriers is 10 to 200 nm [45]. Nanoparticles have a relatively large (functional) surface which is able to bind, adsorb and carry other compounds such as drugs, probes and proteins. The aims for nanoparticle entrapment of drugs are either an enhanced delivery to target cells and/or a reduction in the toxicity of the free drug to non-target organs. Both situations will result in an increase in the therapeutic index [50].

2.4.1   PLGA nanoparticles

Poly(lactic-co-glycolic acid) (PLGA) is a biodegradable polymer synthesized via ring-opening copolymerization of two monomers: the cyclic dimers of glycolic acid and lactic acid. During polymerization, consecutive monomeric units (glycolic or lactic acid) are linked together in PLGA by ester linkages.
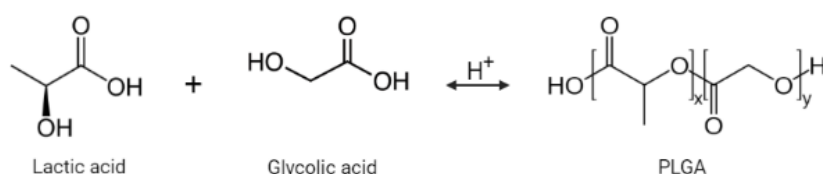
Figure 2.4: PLGA and its monomers

Depending on the ratio of lactide and glycolide, different forms of PLGA can be obtained. They are usually identified with regard to the monomers ratio used so, for example, PLGA 75:25 identifies a copolymer composed of 75% of lactic acid and 25% of glycolic acid [51, 52]. PLGA is one of the most widely used biodegradable polymers for the development of nanomedicines because the cleavage of polymer chains by hydrolysis results in the production of the biodegradable metabolite monomers, lactic acid and glycolic acid [53]. These two metabolites are endogenous and easily eliminated from the body via the

14

Krebs cycle in the form of H_2O and CO_2, so the toxicity associated with the use of PLGA for drug delivery is minimal. The most influencing factors in the degradation of PLGA are the ratio between lactic and glycolic acids in the copolymer chain and the molecular weight of the polymer. By manipulating these two factors, the degradation time of PLGA and, subsequently, the release profile varies. A higher content of lactate results in higher hydrophobicity, leading to lower degradation and slower drug release kinetics, while an increase in the glycolate content contributes to an increase in the hydrophilicity of PLGA being and leads to a much faster degradation and drug release [52, 53].

Amongst all the biomaterials, PLGA has shown immense potential as a drug delivery carrier. Also, PLGA has been regarded as a promising material for drug delivery as it can be surface-tailored with functionalized molecules for site-specific targeting, and is approved by FDA to be used in drug delivery systems [51, 52, 54, 55].

Nanoparticles modification using chitosan

Chitosan is a polysaccharide obtained from the deacetylation of chitin, a polysaccharide found in crustacean shells [56]. It exhibits good biocompatibility and is suitable for the
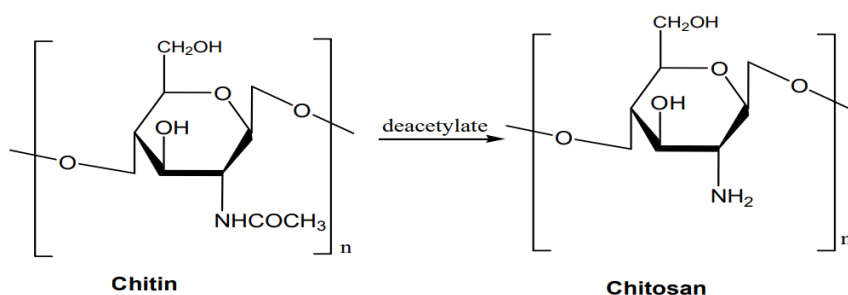
Figure 2.5: Chemical structure showing the preparation of chitosan by deacetylation of chitin

design of targeted drug delivery systems for the treatment of neurodegenerative disorders. It exhibits a positive charge on its surface. Actually, the properties of chitosan make it especially suitable for nasal drug delivery [56, 57]. In fact, chitosan absorbs water from the mucus layer in the nasal cavity, swells and forms a gel-like layer that prolongs the drug's residence time in the nasal cavity, improving its bioavailability [58].

Chitosan coating of PLGA NPs can be achieved by chemical linking to the PLGA or by adsorption due to the electrostatic forces between the positively charged groups of chitosan with the negatively charged group of PLGA. Chitosan also presents good biocompatibility, non-toxicity and biodegradability.

15

2.4.2 Solid lipid nanoparticles

In early 1990s, solid lipid nanoparticles (SLNs) were developed as an alternative to other traditional carriers such as liposomes, emulsions and polymeric nanoparticles, in which the liquid lipid was substituted by a solid lipid [59]. Indeed, SLNs are composed of lipids dispersed in water or in an aqueous surfactant solution, as shown in Figure 2.6. The term lipid is used in a broad sense and includes triglycerides, partial glycerides, fatty acids and waxes. Using a solid lipid instead of liquid lipid is beneficial as it increases the control over the release kinetics of encapsulated compounds and improves the stability of the incorporated ingredients [60, 61].
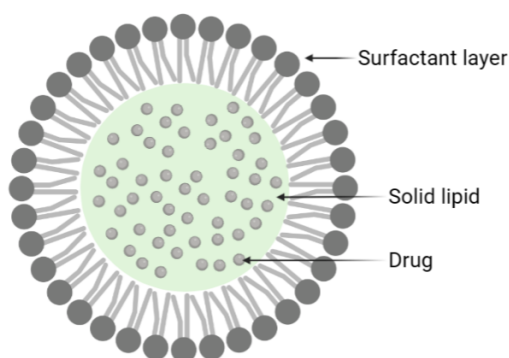
Figure 2.6: Illustration of a solid lipid nanoparticle

A clear advantage of SLN is the fact that, unlike some polymeric nanoparticles, the employment of potentially toxic organic solvents is not needed during the production of SLNs. Furthermore, SLNs offer properties such as small size, large surface area and high drug loading [60, 62]. Their dimensions and the controlled release behavior enable drug protection and their administration through both parenteral and non-parenteral routes, emphasizing the versatility of this carrier [63].

Chapter 3

Nanocarriers for Brain Delivery

Different types of nanocarriers can be used for drug delivery, depending on the application and, thus, their desired properties. In this Chapter, the use of PLGA nanoparticles prepared using the solvent evaporation technique and SLNs manufactured using shear homogenization and ultrasonication will be investigated as potential carriers for a hydrophilic test compound (TC).

3.1 Double Emulsion PLGA Nanoparticles

The encapsulation of hydrophilic compounds in nanoparticles is difficult due to their escape to the external aqueous phase. However, it is possible to entrap hydrophilic compounds using the double emulsion (DE) technique [64]. A DE, also called emulsion of emulsion, is a system in which the dispersed droplets contain even smaller droplets [65]. There are two common types of DE: water-in-oil-in-water (w/o/w) and oil-in-water-in-oil (o/w/o). When an emulsion is w/o/w , water droplets are dispersed within larger oil droplets that are themselves dispersed in an external continuous aqueous phase. In an o/w/o emulsion, the roles of water and oil are switched [65, 66].

One of the possible methods to manufacture NPs is the solvent evaporation technique, which is a top-down method. This means that it is based on the reduction of the dimensions of the starting material by breaking it until the required structures are obtained [67]. Two steps are needed to prepare a w/o/w emulsion:

1. An aqueous solution containing the active ingredient (e.g., the drug) is dispersed in a polymer-containing organic solution to form the water-in-oil (w/o) emulsion

2. The w/o emulsion previously obtained is dispersed in another aqueous phase, such as a polyvinyl alcohol, to form the w/o/w emulsion

For a o/w/o emulsion, the aqueous and the organic phase are used in the opposite way. The organic solution is dispersed in a water solution obtaining an oil-in-water (o/w)

emulsion that will be dispersed in another organic solution. For both emulsions, the
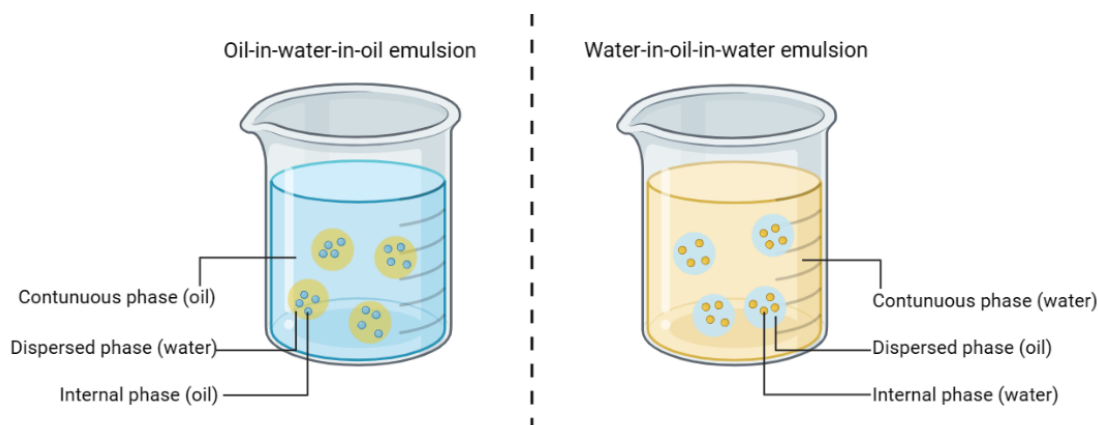

Figure 3.1: Oil-in-water-in-oil and water-in-oil-in-water emulsions

homogenization of the two immiscible phases is achieved by high-speed homogenization and ultrasonication. Once the second emulsion is made, the organic solvent is left to evaporate either by continuous magnetic stirring or in a slow process of reduced pressure. After the solvent has evaporated, the NPs can be collected [66, 68, 69].

3.1.1 Materials

Polyvinyl alcohol 4-88 (Mowiol® 4-88, MW 31000) (PVA), PLGA Resomer® RG 503 H (50:50; MW 24000 – 38000) were purchased from Sigma-Aldrich (St. Louis, MO, USA). Ethyl acetate (99.6%, ACS reagent, MW 88.11) was bought from BioVision (Waltham, MA, USA).

3.1.2 Nanoparticles Preparation

The organic phase was prepared by dissolving 30 mg of PLGA in 1.5 mL of ethyl acetate. After a short time in the vortex (Heidolph Reax Top Vortex Mixer, Heidolph instruments GmbH & Co., Schwabach, Germany), a w/o emulsion was prepared adding to the organic phase 100 uL of ultrapure water. For the TC-loaded PLGA NPs 3 mg of TC were solubilized in the ultrapure water. The suitable masses of polymer (PLGA) and drug (TC) were weighed in a NewClassic MS Analytical Balance from Mettler Toledo (Switzerland). The mixture was shortly vortexed again and sonicated using a UP400S ultrasonic processor from Hielscher (Berlin, Germany). 3 on-off sonication cycles of 10 seconds with an amplitude of 70% were performed. To avoid heating, the falcon was put in a beaker with ice. Then, 2 mL of polyvinyl alcohol (PVA) 1% were added to the previously obtained emulsion. This solution was submitted to vortex and sonication as above. After emulsification, the mixture was poured into a beaker and kept in continuous stirring (Colosquid,

ika®, Magnetic Stirrer) using a magnetic stirrer at 800 rotations per minute (rpm). The stirring was carried on at room temperature until the organic solvent was completely evaporated. A schematic visual description of the method is presented in Figure 3.2.

After the organic solvent's evaporation, the volume of the solution was measured. In
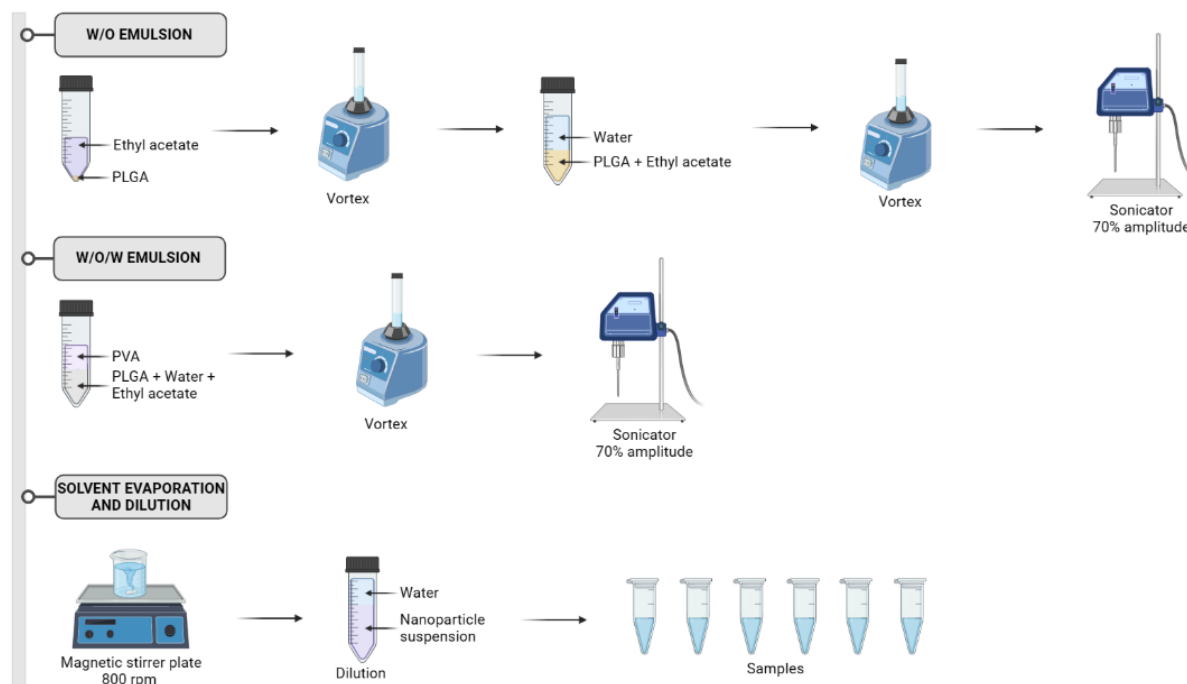
Figure 3.2: Schematic representation of the steps to prepare PLGA nanoparticles

order to have TC at the concentration of 1 mg/mL, the precise amount of ultrapure water to reach the total of 3 mL was added the formulation. The same process was performed for the unloaded NPs. The so obtained mixtures were divided in 10 Eppendorfs with 300 µL each. The samples were incubated at 37°C under gentile agitation to model the in vivo movements and collected at different time points to evaluate over time the NPs' size, polydispersity index (PDI) and zeta potential (ZP) as well as the encapsulation efficacy (EE).

To collect the NPs, the incubated samples were centrifuged (MiniSpin®plus, Eppendorf, Germany) for 15 minutes at 14.500 rpm. To be sure that all the NPs precipitated, the supernatant was collected and centrifuged again for 15 minutes at 14.500 rpm. The pellet was resuspended in 1 mL of ultrapure water.

3.1.3 Characterization of the Nanoparticles

The physicochemical characterization of the NPs was based on the measurements of their size (nm), PDI and ZP (mV). For this purpose, the DLS technique was used. To perform

the measurements, the ZetaSizer Nano ZS equipment (Malven Instruments, UK) was used, and the obtained data were analysed by ZetaSizer software (version 8, Malven).

The amount of drug encapsulated in the NPs was quantified by an indirect method, which consisted of the measurement of the amount of the non-encapsulated drug, that is the drug present in the supernatant. The determination of the non-encapsulated drug was performed using a Synergy 2 Microplate Reader (BioTek, UK) for UV-Vis absorbance measurements and correlated to a calibration curve. The EE was determined using the equation:

$$EE(\%) = \frac{total\ amount\ of\ drug - amount\ of\ free\ drug}{total\ amount\ of\ drug} \times 100 \qquad (3.1)$$

The supernatant obtained from the centrifugation contained free PLGA, PVA and drug. Therefore, the BCA (Bicinchoninic Acid) Protein Assay Kit (Thermo Scientific, Waltham, Massachusetts, USA) was used to enhance the absorbance of the free drug. Using this assay, the absorbance peak is always at a wavelength of $\lambda = 562$ nm.

Dynamic Light Scattering

Dynamic light scattering (DLS), also known as photon correlation spectroscopy or quasi-elastic light scattering, is a technique used to characterize particles, emulsions or molecules which are either dispersed or dissolved in a liquid. This method can provide information about the NPs' size and size distribution [70, 71].

DLS measures the Brownian motion of molecules in solution that arises from their collision with the molecules of the surrounding liquid medium. As a consequence of the motion, if a laser light irradiates the solution, the light will scatter at different intensities in a time-dependent manner due to the continuously changing distances between particles [70, 72]. Indeed, small molecules move faster than larger ones and upon irradiation with light a smaller fraction of light is scattered [73]. Analyzing the variation of intensity over time, the speed of the Brownian motion and hence the particle size can be determined. The size of particles is determined as hydrodynamic radius. The hydrodynamic radius is defined as the radius of a sphere that diffuses at the same rate within the same viscous environment of the investigated particles [72, 74].   In a DLS instrument, the light from a laser is focused on a sample, and when it encounters macromolecules it scatters in all directions. The scattered light is continuously recorded and quantified by a detector whose output is digitized by a photon-counting system. The number of photons hitting the detector changes over time and is sent to a digital autocorrelator, which correlates intensity fluctuations of scattered light with the time to determine how rapidly the intensity of light is fluctuating. Using the autocorrelation, it is possible to calculate the diffusion coefficient (D), which can be used to determine the hydrodynamic radius (R) of the corresponding
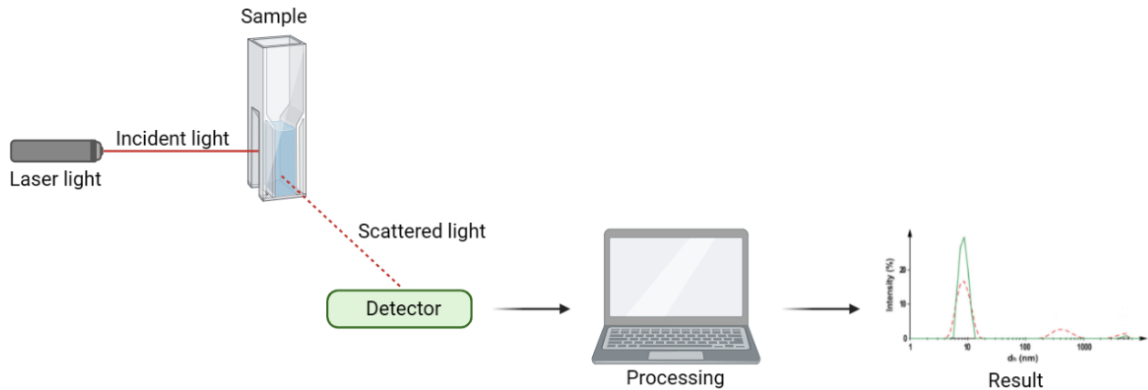
Figure 3.3: Dynamic light scattering (DLS) processing

spherical particles according to the Stokes-Einstein equation:

$$D = \frac{k_B T}{6\pi\eta R} \tag{3.2}$$

In the equation, k_B is Boltzmann's constant, T is the temperature, which for most measurements is kept constant, and η is the known viscosity of the suspending medium [71, 75]. A DLS instrument also returns the PDI of the measured particles. Indeed, there might be particles with a distribution of sizes rather than particles of a single size [75]. Thus, the particles in the distribution have different translational self-diffusion coefficients. The polydispersity index value is useful for identifying the presence of aggregates, too [70].

When a particle encounters a solution, it gets an electrical charge on its surface. In particular, when a particle is dispersed, an electrical double layer – namely, the electric double layer (EDL) - develops on its surface. The inner layer, called Stern layer, consists of ions with an opposite charge to the one of the particle and that are strongly attached to the particle's surface; the other area, called Diffuse layer, ions are less firmly attached. Within the Diffuse layer there is a boundary: the Slipping plane. Any ions inside the Slipping plane move together with the particle when it moves in the solution, but any ions outside it will not. The electrical potential in the Slipping plane is known as the electrokinetic potential or, more commonly, ZP. Therefore, the ZP reflects the potential difference between the EDL of particles and the layer of dispersant around them at the Slipping plan. ZP cannot be measured directly and is thus deduced using the electrophoretic mobility technique. The technique consists in placing the sample in a two-electrode cuvette and applying an electric potential. This allows to measure the movement of particles towards the opposite charged electrode, called electrophoresis.

The electrophoretic mobility (μ_e) of the particles is first calculated as $\mu_e = \frac{V}{E}$, where V is the particle's velocity (μm/s) and E is the electric field strength (Volt/cm). The particle's velocity and the strength of the electric field are both known quantities. ZP is

21

then calculated using the Helmholtz-Smoluchowski equation

$$\mu_e = \frac{\varepsilon_r \varepsilon_0 \zeta}{\eta} \tag{3.3}$$

with ε_r dielectric constant, ε_0 permittivity of vacuum, ζ ZP and η viscosity at experimental temperature. This equation is a modification of Henry's equation and is used when the thickness of the EDL is much smaller compared to the particle radius, which is the case of most pharmaceutical preparations. The ZP value gives an indication of the stability of the system: if particles in suspension have a large negative or positive zeta potential, they will tend to repel each other. On the other hand, if the particles have a low ZP there will be no force to prevent the particles from moving closer and, eventually, aggregate [76].

Spectrophotometry

Spectrophotometry is a technique that allows measuring the absorbed light of a solution. This method is used to quantify the presence of an analyte in a sample. In most cases, the analyte of interest absorbs light at a specific wavelength. The quantity of absorbed light is proportional to the amount of analyte [77]. Absorbance scans are depicted with wavelengths in nanometers (nm) on the X-axis and the amount of light absorbed on the Y-axis. The absorption spectrum of a compound is useful for both qualitative (identification) and quantitative (concentration) analysis.

There are two main propositions that define the light absorption's laws. Lambert's law asserts that the proportion of incident light absorbed by a transparent medium is independent of the intensity of the light (Lambert, 1760). Therefore, consecutive layers with the same thickness will transmit the incident energy in an equal proportion. This is defined by the equation

$$T = \frac{I}{I_0}, \tag{3.4}$$

where T is the transmittance, I the intensity of the transmitted light and I_0 the intensity of the incident light. Beer's law states that the light's absorption is directly proportional to the concentration of the absorbing medium and the thickness of that medium (Beer, 1852). The combination of the two laws, the Beer-Lambert law, asserts that

$$A = logT = log\frac{I}{I_0}, \tag{3.5}$$

where A is the absorbance, I the intensity of the transmitted light and I_0 the intensity of the incident light. The Beer-Lambert law also provides a measure of the uniform concentration c of a light-absorbing solute. When a sample of that solution is enclosed within a cell with a path-length X, with parallel, planar and non-absorbing walls at the wavelength of interest, its absorbance is given by the equation

$$A = \varepsilon c X \tag{3.6}$$

22

Each compound in a solution absorbs or transmits light over a certain wavelength. To measure absorbance, the sample in the plate is illuminated by a light beam with a specific intensity which passes through the sample. On the opposite side of the microplate compared to the light source, is located a light detector. The light detector measures how much of the total light intensity is transmitted and at which wavelengths. In fact, the amount of light that does reach the detector is absorbed by the sample [77].
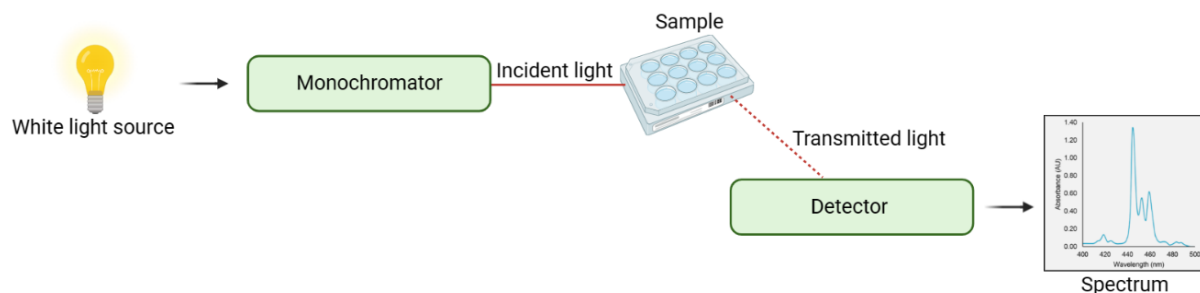
Figure 3.4: Absorbance measurement

To study the EE of the NPs, the BCA Protein Assay was used (Appendix A) and, for this reason, the absorbance values corresponding to a wavelength of 562 nm were considered. For this purpose, a Synergy 2 Microplate Reader (BioTek, UK) was used.

3.2 PLGA Nanoparticles produced by Single Emulsion

A single emulsion consists of droplets dispersed in a different fluid, often stabilized with a surfactant. Single emulsions are produced using two immiscible liquids. In particular, two types of single emulsion are possible. An oil-in-water (o/w) emulsion consists of an oil phase dispersed into water, which is the continuous phase. In contrast, a water-in-oil (w/o) emulsion consists of a water phase dispersed into a continuous oil phase. As for the DE, the two phases are homogenized using high-speed homogenization or ultrasonication.

Single emulsion PLGA NPs were prepared using an organic solvent in which TC was soluble. In addition, only solvents non-miscible with water and in which PLGA could be dissolved were considered. Chloroform was chosen as the organic solvent.

3.2.1 Materials

Polyvinyl alcohol 4-88 (Mowiol® 4-88, MW 31000) and PLGA Resomer® RG 503 H (50:50; MW 24000 – 38000) were purchased from Sigma-Aldrich (St. Louis, MO, USA). Chloroform was purchased from Honeywell (Charlotte, NC, USA).

3.2.2 Nanoparticles Preparation

30 mg of PLGA were dissolved in 1.5 mL of chloroform. After a short time in the vortex (Heidolph Reax Top Vortex Mixer, Heidolph instruments GmbH & Co., Schwabach, Germany), 2 mL of PVA 1% were added to the previously prepared organic phase. The mixture was sonicated (UP400S Ultrasonic Processor, Hielscher, Berlin, Germany) for 3 on-off cycles of 10 seconds with an amplitude of 70%. To avoid heating, the falcon was put in a beaker with ice. After emulsification, the mixture was poured into a beaker and kept in continuous stirring (Colosquid, ika®, Magnetic Stirrer) using a magnetic stirrer at 800 rpm. The stirring was carried on at room temperature until complete organic solvent evaporation.

Once the organic solvent was completely evaporated, the NPs' size, PDI and ZP were measured after a 1:10 dilution in ultrapure water.

3.2.3 Experimental Parameters for the Production of Single Emulsion PLGA Nanoparticles Using Chloroform

To obtain the desired properties (i.e., size, PDI and ZP) for the NPs, different experimental parameters have been tested. The size of the NPs is especially important for this application, so different tests were performed to achieve a NPs' size as close as possible to 200 nm. Table 3.1 summarizes the different experimental parameters. In particular, the parameters that were varied are the ratio between chloroform and PVA, the PVA concentration and number and the duration of the sonication cycles.

Batch	Chloroform [mL]	PVA concentration [%]	PVA [mL]	# of cycles	Cycles' duration [sec]
c1, c2	1.5	1	2	3	10
c3, c6	0.5	1	2	3	10
c4, c7	1.5	1	3	3	10
c5, c8	3	1	4	3	10
s1	3	1	4	1	10
s2	3	1	4	3	20
s3, s4	3	1	4	6	10
s5	3	1	4	12	10
p1	3	5	4	3	10

Table 3.1: Different experimental parameters for the preparation of single emulsion PLGA NPs

3.3 PLGA Nanoparticles produced by Single Emulsion Modified with Chitosan

Unloaded PLGA NPs were prepared to implement nose-to-brain delivery. For this purpose, chitosan was used. Control NPs, without chitosan, were prepared following the same protocol.

3.3.1 Materials

Polyvinyl alcohol 4-88 (Mowiol® 4-88, MW 31000), PLGA Resomer® RG 503 H (50:50; MW 24000 – 38000) and acetic acid ($\geq$98%, MW 60.05) were purchased from Sigma-Aldrich (St. Louis, MO, USA). Ethyl acetate (99.6%, ACS reagent, MW 88.11) was bought from BioVision (Waltham, MA, USA). Chitosan (MW 248 kDa, degree of deacetylation 93) was obtained from Altakitin (Aveiro, PT).

3.3.2 Preparation of Single Emulsion PLGA Nanoparticles Modified with Chitosan

To prepare both the control NPs and the NPs modified with chitosan, the organic phase was prepared dissolving 10 mg of PLGA in 0.5 mL of ethyl acetate. Only for the chitosan-modified NPs, a solution of 1 mg of chitosan in 66 µL of acetic acid 1% was prepared. To the solution of chitosan in acetic acid was added 934 μL of PVA 1%. This solution was added drop-by-drop to the organic phase. For the control NPs, 1 mL of PVA 1% was added to the prepared organic phase drop-by-drop. After 30 seconds in the vortex (Heidolph Reax Top Vortex Mixer, Heidolph instruments GmbH & Co., Schwabach, Germany), both preparations were emulsified using a probe sonicator (UP400S ultrasonic processor, Hielscher, Berlin, Germany) for 3 on-off cycles of 10 seconds with an amplitude of 70%. To avoid heating, the falcons were put in a beaker with ice. The emulsions were then transferred in two beakers and placed on a magnetic stirrer plate (Colosquid, ika®, Magnetic Stirrer) at 800 rpm. The stirring was carried on at room temperature until the organic solvent was completely evaporated. Once the organic solvent was completely evaporated, the NPs' size, PDI and ZP were measured after a 1:10 dilution in ultrapure water.

3.4 Solid Lipid Nanoparticles

Many different techniques and lipids can be used to manufacture SLNs. In this experimental work, SLNs were produced combining the shear homogenization and the ultrasonication methods.

According to these methods, both the lipid phase and the aqueous phase are heated

to a temperature above the lipid's melting point. The aqueous phase is then added to the lipid melt and the mixture is homogeneously dispersed using a high-shear mixer. An oil in water (o/w) emulsion is formed due to the shear of intense turbulent eddies. High-speed stirring is followed by ultrasonication, which breaks the droplets in order to generate droplets of nanometric size. Finally, the nanoparticles are left to cool down, allowing the lipid crystallization.

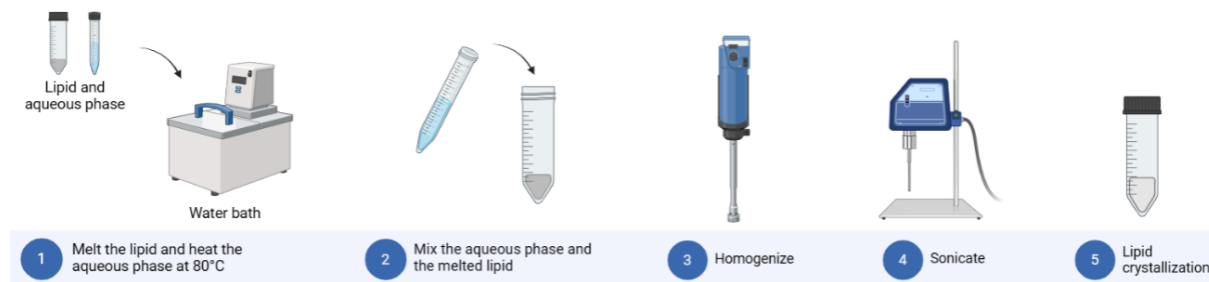If ultra-sonication is performed without implementing the high-shear mixing proce-

Figure 3.5: Schematic representation of the steps to prepare solid lipid nanoparticles

dure, the produced SLNs will have a broad distribution, supposedly because the sonication energy is not transferred equally in the batch. For this reason, to achieve SLNs' dispersions with narrow particle distributions, the conjunction of high-speed stirring and ultra-sonication has been widely used [78].

3.4.1 Materials

Compritol 888 ATO was purchased from Gattefossé SAS (Saint-Priest, Cedex, France). Pluronic® F-127 (powder, BioReagent) was purchased from Sigma-Aldrich.

3.4.2 Preparation of Solid Lipid Nanoparticles

The lipid phase was prepared weighting different amounts of Compritol 888 ATO. The aqueous phase was prepared by adding 2.175 mL of Pluronic F-127 10%. Compritol 888 ATO's melting temperature is 78°C, so both phases were warmed in a water bath at 80°C until the lipid was completely melted. Then, the aqueous phase was added to the lipid phase, and the obtained preparation was homogenized using a high-shear mixing device (ULTRA-TURRAX® DI 25 Basic, Yellow Line) for 1 minute at 13.500 rpm. After, the emulsion was sonicated using a probe sonicator (UP400S Ultrasonic Processor, Hielscher, Berlin, Germany) for 5 minutes with an amplitude of 80%. To allow the lipid crystallization, the emulsion was let to cool down in a beaker with ice in continuous stirring (Colosquid, ika®, Magnetic Stirrer) at 100 rpm. The stirring was

carried on at room temperature for 1 hour.

In order to characterize the obtained SLNs in terms of size, PDI and ZP, a dilution in ultrapure water was performed according to Table 3.2.

Several amounts of lipid were tested to check if it was possible to obtain SLNs with the desired properties using a lower amount of lipid and, thus, the drug. The different amounts of lipid used and their respective dilution are summarized in Table 3.2.

Batch number	Lipid [mg]	Aqueous phase [mL]	Dilution factor
b1, b2	250	2.175	1:100
b3, b4	25	2.175	1:10
b5, b8	50	2.175	1:10
b6, b7	100	2.175	1:10

Table 3.2: Different experimental parameters for the preparation of SLNs

It was not possible to decrease the amount of aqueous phase (i.e., Pluronic 10%) because of the ULTRA-TURRAX®. Indeed, the high-shear mixing device requires at least 2.175 mL of liquid to work properly.

3.5 Results

3.5.1 PLGA Nanoparticles Produced by Double Emulsion

The size, PDI and ZP over time of the PLGA NPs produced by the double emulsion method using PVA as stabilizer are shown, respectively, in Figure 3.6, 3.7 and 3.8.
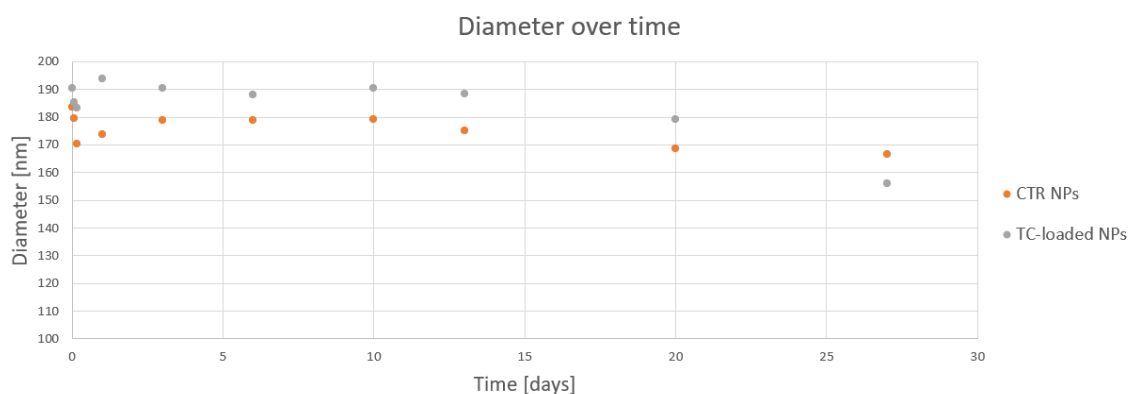

Figure 3.6: Double emulsion PLGA nanoparticles diameter

The size, PDI and ZP only at time zero was calculated as the average of two batches.
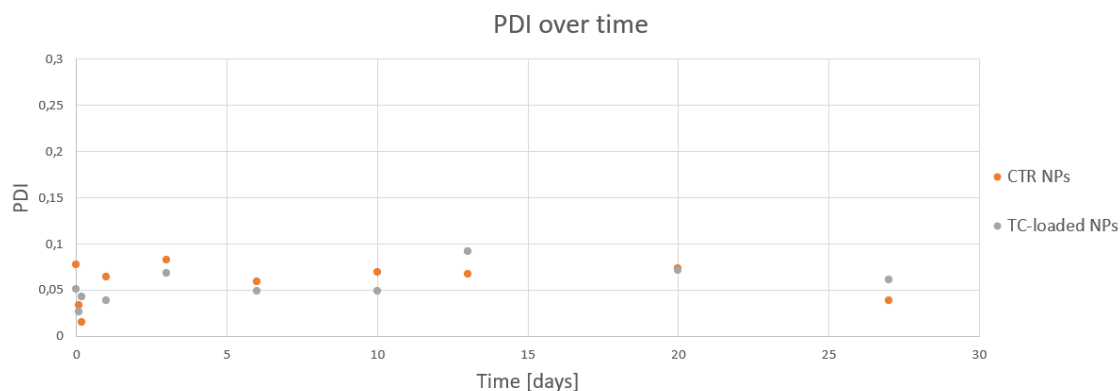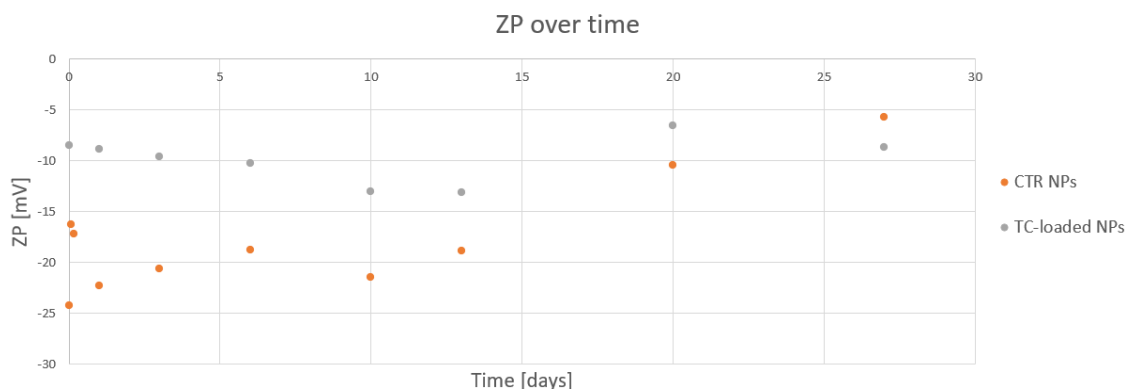
Figure 3.7: Double emulsion PLGA nanoparticles PDI

Figure 3.8: Double emulsion PLGA nanoparticles ZP

At time zero, the control NPs revealed to have an average size of 185.65±1.95 nm, a PDI of 0.052±0.026 and ZP of -22.6±1.6 mV; while the loaded NPs exhibited a size of 187.75±2.85 nm, a PDI of 0.071±0.019 and ZP of -7.81±0.69 mV. The size of the NPs did not change in the first 13 days of the study. However, at 20 and 27 days, it is possible to notice a drop in their size. The control NPs' size decreased from 175.2 nm at 13 days to 168.5 nm at 20 days and, finally, 166.6 nm at 27 days. For the loaded NPs the reduction of the size is even clearer: it changed from 188.4 nm at 13 days to 179.3 nm at 20 days and 156.1 nm at 27 days. The PDI was lower than 0.1 at every time point, suggesting that the NPs are monodispersed [72].

The value of the ZP obtained for the control NPs at time 0 was -22.6±1.6 mV, accordingly to what was expected. In fact, as reported in other studies [79, 80], the ZP of PLGA NPs is expected to be negative and with an absolute value around 20 mV. Those results are encouraging, since the stability of NPs is directly proportional to the absolute value of ZP. Thus, the values obtained for the ZP indicate that strong repulsive forces

28

were formed between the NPs, which were, therefore, stable over 13 days [80]. The ZP of the loaded NPs has a lower negative charge. The difference between the ZP values of the control NPs and the loaded NPs indicates that a certain amount of the drug, which has a positive charge, is probably located on the surface of the NPs. Nevertheless, for both loaded and unloaded NPs, unexpected results were obtained at 2 and 4 hours and 20 and 27 days. To better understand the ZP fluctuation, this experiment must be repeated. The result could be due to the measurement cuvettes, that may not have been in the proper condition at the moment of the measurements.

The average EE was 36.67±4.68 %.

3.5.2   Single Emulsion PLGA Nanoparticles Using Chloroform

The firstly prepared single emulsion PLGA NPs, that were made using 1.5 mL of chloroform and 2 mL of PVA 1%, turned out to have a mean size of 348.80±20.93 nm (Table 3.3).

PLGA NPs were later manufactured using chloroform and PVA 1% in different proportion, so that the best combination of the two could be found. The number of sonication cycles and their duration were maintained the same as previously (i.e., three cycles on/off of 10 seconds). The results of these tests are summarized in 3.3.

Batches composition	Diameter $\pm$ SD [nm]	PDI $\pm$ SD	Zeta potential $\pm$ SD [mV]
30 mg PLGA, 1.5 mL chloroform, 2 mL PVA 1%	348.80 $\pm$ 20.93	0.186 $\pm$ 0.002	-9.14 $\pm$ 0.70
30 mg PLGA, 0.5 mL chloroform, 2 mL PVA 1%	400.77 $\pm$ 29.26	0.443 $\pm$ 0.149	-22.83 $\pm$ 4.03
30 mg PLGA, 1.5 mL chloroform, 3 mL PVA 1%	311.05 $\pm$ 5.02	0.121 $\pm$ 0.051	-22.00 $\pm$ 0.12
30 mg PLGA, 3 mL chloroform, 4 mL PVA 1%	293.13 $\pm$ 22.07	0.287 $\pm$ 0.101	-23.1 $\pm$ 0.52

Table 3.3: Results obtained varying the amount and proportion of chloroform and PVA 1%

The use of chloroform and PVA in different amounts and proportions allowed to reduce the size of the NPs. The best results were obtained using 3 mL of chloroform and 4 mL of PVA 1%. Even though the mean diameter of these NPs was the lowest among all the types of NPs produced, it was still not adequate for the application.

Different tests were then conducted starting from the best NPs obtained until that time (i.e., NPs prepared using 3 mL of chloroform and 4 mL of PVA 1%) and modifying other parameters of the NPs' production. Thus, experiments were performed varying the number of sonication cycles and their length, in order to understand the influence they had on the NPs' characteristics. In addition, tests were conducted increasing the PVA concentration from 1% to 6%. In fact, it has been reported that increasing the concentration of PVA, the mean particle size decreases [81]. This is attributed to the fact that at concentrations higher than 2.5% PVA exists in an aggregated form, which enhance its surfactant activity [81].

Table 3.4 sums up the size, PDI and ZP of the NPs whose experimental parameters can be found in Table 3.1.

PVA concentration	Sonication cycles	Diameter [nm]	PDI	Zeta potential [mV]
1%	1 cycle of 10 sec	362.60	0.397	-22.00
1%	3 cycles of 20 sec	245.10	0.258	-16.90
1%	6 cycles of 10 sec	238.10	0.052	-21.20
6%	3 cycles of 10 sec	360.10	0.175	-6.87

Table 3.4: Results obtained using 3 mL of chloroform and 4 mL of PVA, varying the concentration of PVA and the number and duration of sonication cycles

From the results in Table 3.4, it is possible to state that the PVA concentration did not make a difference in the particles' characteristics compared to the previous studies. In contrast, the number and the duration of the sonication cycles did. The best results for what it concerns the size of the NPs were those obtained using six cycles of sonication ten seconds and three cycles of sonication twenty seconds long.

Figure 3.9: Diameter distribution and ZP of single emulsion PLGA NPs prepared using 3 cycles of 20 seconds (A, B) and 6 cycles of 10 seconds (C, D)

Comparing the size and the ZP distribution, the NPs made using the sonicator for six on-off cycles 10 seconds long have a better profile to the ones obtained using twelve on-off cycles of 10 seconds. These particles are less polydispersed and the ZP is more similar over the three measurements than in the other case, as shown in Figure 3.9.

The number of sonication cycles was then increased to twelve to check if it was possible to obtain even smaller NPs, but this did not happen. Indeed, the size of the NPs was a very similar to the one of the NPs prepared using six cycles of 10 seconds, that is 242 nm
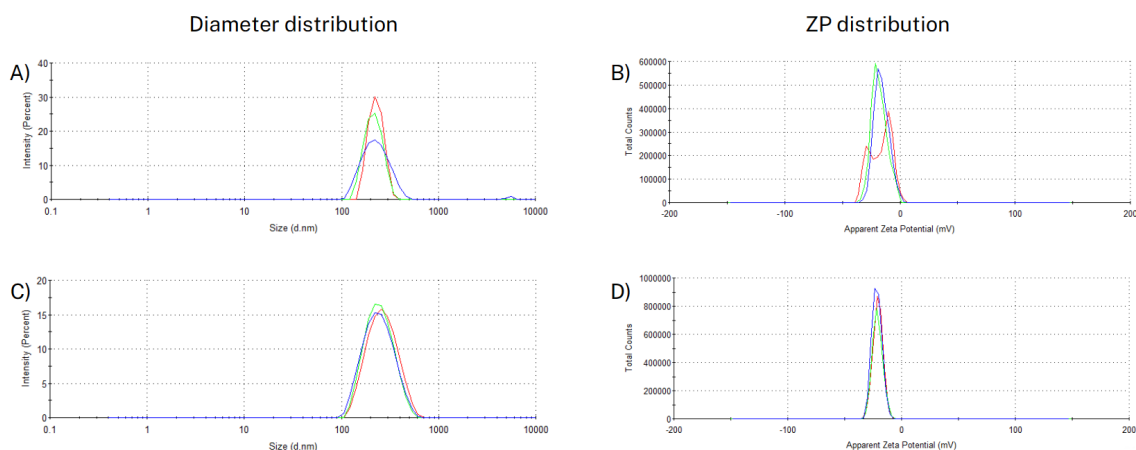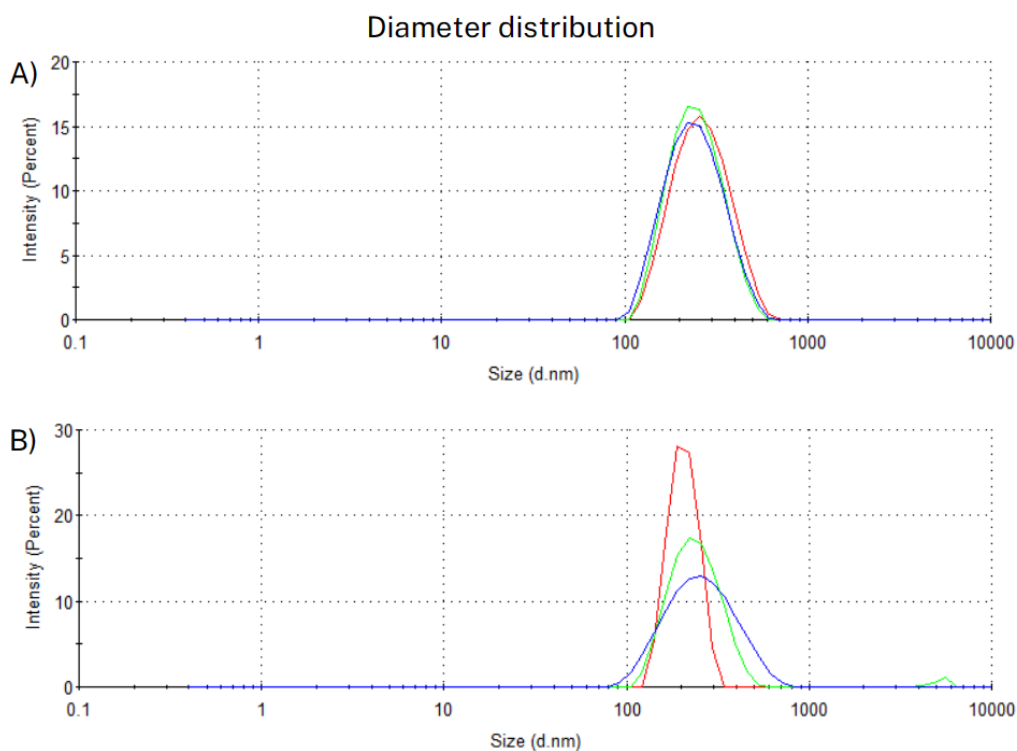
Figure 3.10: Diameter distribution of single emulsion PLGA NPs prepared using 6 cycles of 10 seconds (A) and 12 cycles of 10 seconds (B)

compared to 238 nm, as shown in Figure 3.10.

The best results were thus obtained using 3 mL of chloroform, 4 mL of PVA 1% and six sonication cycles of 10 seconds. However, from some measurements emerged the presence of aggregates, as shown in Figure 3.11.
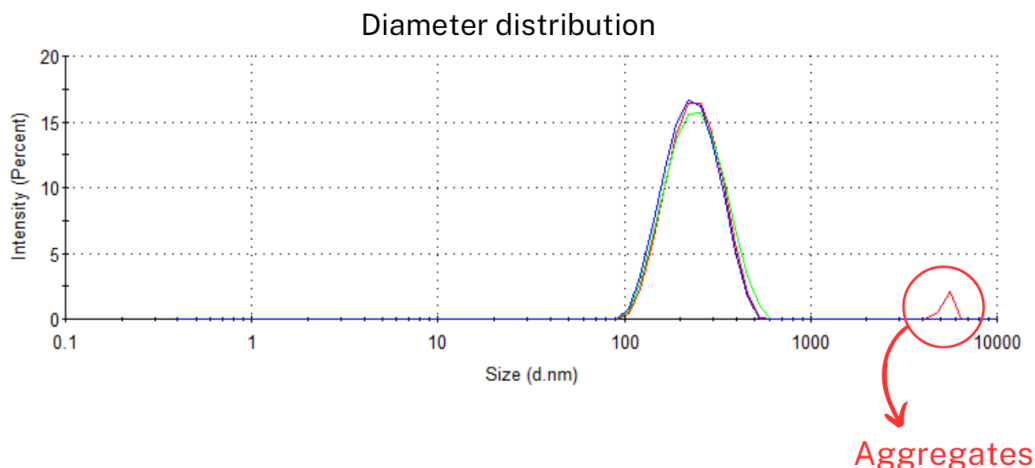
Figure 3.11: Presence of aggregates in the NPs prepared using 6 on-off cycles of sonication 10 seconds long

3.5.3 PLGA Nanoparticles Modified with Chitosan

To improve the brain delivery, PLGA NPs were modified with chitosan to provide mucoadhesive properties to the NPs themself. The comparison between the chitosan-modified PLGA NPs and the control NPs is shown in Table 3.5.

	Average diameter ± STD [nm]	Average PDI ± STD	Average zeta-potential ± STD [mV]
Control NPs	178.70 ± 26.60	0.126 ± 0.069	-8.825 ± 0.595
Chitosan-modified NPs	199.05 ± 24.75	0.156 ± 0.044	6.295 ± 0.355

Table 3.5: Diameter, PDI and ZP of chitosan-modified and control NPs

The size, PDI and ZP of the NPs were expected [82]. The slightly bigger size of the chitosan-modified NPs was foreseen as well [83]. For what it concerns the ZP, a higher ZP in the modified NPs was predictable due to the positive charge of chitosan.

Figure 3.12 confirms the good results obtained for the PDI of the NPs.

3.5.4 Solid Lipid Nanoparticles

Table 3.6 summarizes the size, PDI and ZP of the SLNs produced using different amounts of lipid.

The firstly prepared SLNs were produced using 25 mg of lipid. Their average size and PDI turned out to be, respectively, 368.40±17.90 nm and 0.260±0.069. These results were not in line with the requirements of the application.

Increasing the amount of lipid to 50 mg, the size of the particles decreased to an average of 236.55±1.95 (Figure 3.13). The PDI did not suffer a great change, being 0.277±0.011.
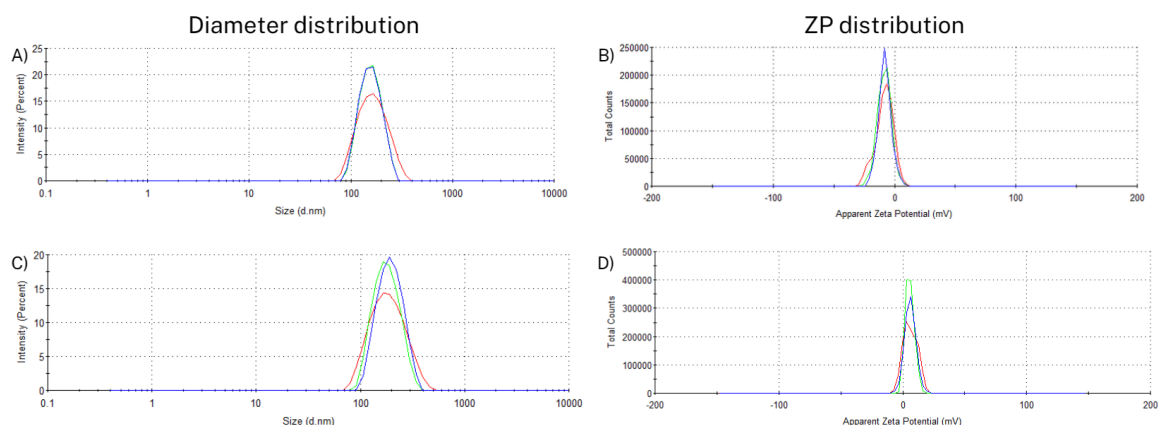
Figure 3.12: Diameter distribution and ZP of control (A, B) and chitosan-modified (C, D) NPs

	Average diameter ± STD [nm]	Average PDI ± STD	Average zeta-potential ± STD [mV]
25 mg Compritol	368.40 ± 17.90	0.260 ± 0.068	-23.00 ± 3.30
50 mg Compritol	236.55 ± 1.95	0.277 ± 0.011	-21.10 ± 0.30
100 mg Compritol	233.07 ± 42.73	0.275 ± 0.121	-20.07 ± 5.93

Table 3.6: Diameter, PDI and ZP of SLNs

Also, one of the three measurements has a way wider distribution than the two others. Using 100 mg of lipid, the results were not reproducible. The average size was of 233.07 nm with a STD of 42.73 nm. Between the three batches, the lowest size was 174.7 nm and the highest was 275.8 nm. The PDI ranged from 0.114 to 0.407. The same happened for the ZP, which changed from -15.1 mV to -28,4 mV.

Considering the different amounts of lipid tested, the best results were obtained using 50 mg of Compritol 888 ATO. This amount of lipid allowed us to obtain reproducible results, with a particle size close to 200 nm and an acceptable PDI.

Figure 3.13: Diameter distribution of SLNs produced using 50 mg of Compritol

Chapter 4

Discussion

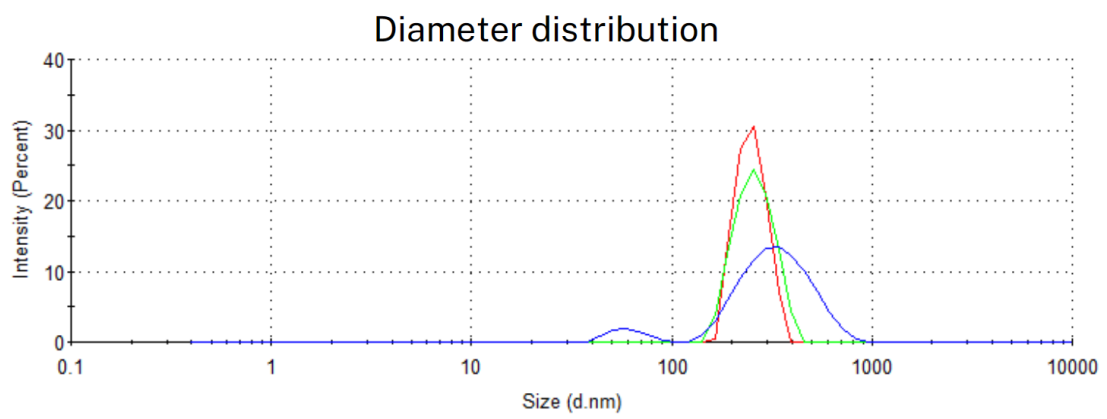## 4.1 Double Emulsion PLGA Nanoparticles

The prepared double emulsion PLGA nanoparticles showed a low entrapment efficacy compared to other studies. E. Cohen-Sela et al. were able to encapsulate hydrophilic molecules in double emulsion PLGA NPs obtaining an EE of 55.1±7.4% [84]. Anyway, J. M. Barichello et al. obtained a poor encapsulation in PLGA NPs for two different hydrophilic drugs (EE of 12.1±1.3% and 9.4±1.3%). In fact, hydrophilic drugs might suffer of low affinity with the polymer used to produce the NPs (i.e., PLGA), resulting in a poor interaction between the two. Due to the poor interaction, the drug will diffuse from the organic phase to the aqueous phase during the emulsification process [86]. However, the NPs have satisfactory sizes, lower than 200 nm, which prevent their filtration by the liver and increase their chance to efficiently cross the BBB. Using the double emulsion solvent evaporation technique, K. P. Cruz et al. and E. Cohen-Sela et al. obtained a higher particles' diameter, respectively of 305.5 nm and 223 nm [84, 85]. In addition, the NPs have a low PDI, making them monodispersed. This is a favorable result, because it means that all the NPs have a size very close to the average one. In particular, in all the measurements the PDI was lower than 0.1, which did not happen in other studies. R. Scherließ and J. Janke and K. P. Cruz et al. reported, respectively, a PDI of 0.13 and 0.129 for NPs prepared using the double emulsion solvent evaporation technique [85, 87]. For what it concerns the ZP, the results were expected due to the negative charge of PLGA and the positive charge of TC. Nevertheless, more tests are required to investigate why the ZP after 2 and 4 hours and 20 and 27 days changed drastically. In fact, the ZP affects the stability of the NPs: a significant positive or negative ZP value (±30 mV) indicates excellent physical stability due to the presence of electrostatic repulsion forces between individual particles. Conversely, a lower ZP value induces instability, such as particle aggregation [88]. Additionally, the ZP of the TC-loaded NPs show some differences when compared to the ZP of the unloaded NPs, suggesting that the encapsulation of this

compound can provoke changes in the particles' surface charge. This can be explained by the distribution of TC within the NPs: if the compound, which has a positive charge, is close to the NPs surface, the ZP increases.

4.2 Single Emulsion PLGA Nanoparticles Using Chloroform

Using 3 mL of chloroform, 4 mL of PVA 1% and six on-off sonication cycles of 10 seconds it was possible to obtain reproducible NPs with a mean diameter of 239.4±2.3 nm, a PDI of 0.1075±0.0295 and a ZP of -19.30±0.15 mV. The size is slightly above 200 nm, but is lower than the one obtained at the beginning (i.e., 362.6 nm, obtained with 3 mL of chloroform, 4 mL of PVA 1% and one sonication cycle of 10 seconds). A decrease in the particles' size due to an increase of the sonication time has been reported in other studies [89, 90]. However, it has also been shown that a benefit can be obtained only up to a certain sonication time, depending on the study. The initial decrease of the size can be attributed to the energy of the emulsification process, that creates the condition to prevent coalescence of the emulsion droplets and results in the formation in smaller droplets, which led to smaller NPs. The subsequent increase of the size may be due to a de-emulsification process or the generation of surface charge that leads to the agglomeration of the particles. These results improved also respect to the PLGA NPs prepared by the single emulsion solvent evaporation technique by M. Alkholief et al. [91], whose average size was of 328.1±24.4 nm. The PDI decreased as well and is very similar to the one obtained by M. Alkholief et al., that is, respectively, 0.1075±0.0295 and 0.096±0.079 [91]. This implies that all the NPs have a size very similar to the average one. The ZP was the one expected for PLGA NPs. In fact, PLGA has a negative charge. Despite these promising results, the protocol used to produce PLGA NPs using chloroform needs some adjustments because of the presence of aggregates. For example, a different surfactant might be used. A. Musyanovych et al. used sodium dodecyl sulfate and cetyltrimethylammonium chloride as a stabilizer for the preparation of PLGA NPs using chloroform as organic solvent. In that study, the NPs obtained using sodium dodecyl sulfate and cetyltrimethylammonium chloride had, respectively, a mean diameter of 121 and 80 nm and a PDI of 0.10 and 0.12. The presence of aggregates was not reported [92]. Another possible option is to replace chloroform with another organic solvent. This possibility, however, is strictly depending on the solubility of the compound under investigation in the solvent itself.

4.3 Single Emulsion PLGA Nanoparticles Modified with Chitosan

NPs modified with chitosan, designed for nose-to-brain delivery, showed auspicious results. Their average size is lower than 200 nm and their PDI is close to 0.15, making them suitable for this application. The higher average mean size of the chitosan-modified NPs was expected due to the presence of chitosan itself, as shown by Y. Wang et al. and B. Lu et al. [93, 94]. The size of the obtained NPs is lower than the one obtained by Y. Wang et al. However, using nanoprecipitation, B. Lu et al. obtained pure PLGA NPs with a size of 132.8±1.5 nm and chitosan-modified NPs with an average diameter ranging from a minimum of 140.5±2.4 nm to a maximum of 172.7±3.2 nm, depending on the amount of chitosan used. In particular, the higher the amount of chitosan, the higher the average diameter. The PDI of the control NPs is lower than the one obtained by B. Lu et al., that is 0.126±0.069 compared to 0.155±0.03 obtained. However, B. Lu et al. obtained a lower PDI for the chitosan-modified NPs: 0.144±0.06 compared to 156±0.044. The ZP of the unmodified PLGA NPs was negative (-8.825±0.595 mV) for the presence of the carboxyl groups of PLGA molecules. This result is in accordance to the other studies [93, 94]. The positive ZP of the chitosan-modified PLGA NPs was expected as well, due to the fact that chitosan is a positively charged polysaccharide. Even this result is in agreement with the results of the other studies [93, 94]. In particular, it indicates that chitosan had been successfully coated PLGA NPs. In addition, the chitosan-modified NPs are expected to interact *in vivo* with the nasal mucosa, due to their opposite charge. Electrostatic interactions will create because of the positive charge of chitosan and the negative charge of the nasal mucosa molecules, resulting in the adhesion of the NPs to the mucosa and in their prolonged residence time in it. Moreover, the positive charge of chitosan is responsible for its ability to enhance the permeability of the nasal epithelium. Again, bonds will form due to electrostatic interaction between chitosan and the mucus, leading to the reversible opening of the junction in the olfactory epithelium and the subsequent increased permeation of the NPs [95, 96].

4.4 Solid Lipid Nanoparticles

The best SLNs that were possible to obtain by reducing the amount of lipid to use are those prepared with 50 mg of lipid. However, it is not possible to reproduce the size that can be obtained using 250 mg of lipids. C. Righeschi et al. showed the effect of the sonication time on the size of SLNs [97]. In their case, the SLNs prepared using 5 minutes sonication had an average size of 333±1 nm, while using 15 minutes of sonication the size of the SLNs decreased to 241±9 nm. The size of the SLNs produced using 50 mg of lipid was lower than the one obtained by C. Righeschi et al. (236.55±1.95 nm) but increasing the sonication time could be an approach to try to obtain smaller particles. Moreover,

many different types of lipids as well as various emulsifiers and their combination can be used to produce SLNs. For this reason, the production of SLNs using lipids other than Compritol 888 ATO might be studied. For example, N. M. Morsi et al. produced SLNs with an average diameter of 123 nm using glyceryl monostearate as lipid and a mixture of Tween 80 and Pluronic F68 in a ratio 1:1 as surfactant [99] and G. D. Kalaycioglu and N. Aydogan were able to obtain SLNs with a size of 148.0±1.3 nm using stearic acid as lipid and Pluronic F127 as stabilizer [100]. The ZP obtained in this project was of -21.10±0.30 mV. The negative surface charge was expected since a negatively charged lipid and a neutral surfactant were employed. The result is in accordance to C. Freitas and R. H. Muller that produced SLNs using Compritol 888 ATO with a ZP of -24.7 mV [97, 98]. It is also confirmed by N. M. Morsi et al., who prepared SLNs with different formulations, and whose ZP ranged from –10.05±0.56 mV to -22.92±4.51 mV [99].

Chapter 5

Future Perspectives

The success of a neurodegenerative disease therapy depends not only on the pharmacokinetic and pharmacodynamic activity of the therapeutic agent but also on its bioavailability and toxicity. It is therefore important to develop nanocarriers with a low toxicity that allow to enhance the therapeutic activity of the compound.

A growing effort has been applied to find novel approaches for the treatment of neurodegenerative diseases and, in recent years, a growing number of studies was published, focusing on the research and development of NPs as drug delivery systems to target the brain. Nanoparticles are promising candidates for drug delivery as they present numerous advantages such as protecting the drugs from the macrophage uptake, thus enhancing the blood circulation time, and providing an increased and controlled release into the specific final target.

PLGA NPs are very versatile and can be modified to achieve different types of drug administration. For this reason, in this work, they were proposed as a drug delivery system for drugs that can fight AD along with solid lipid nanoparticles. So, in the future, the studies initiated in this work should continue to be investigated to a deeper level. For example, the stability over time of the single emulsion PLGA NPs and the SLNs should be investigated. This is necessary to confirm that the properties of the particles, such as their size and surface chemistry, do not change with time. It is also useful to confirm that aggregates did not appear. If the presence of aggregates occurs, different surfactants and/or organic solvents can be employed. Surfactants and organic solvents can be used in different proportion in order to obtain NPs with various characteristics. In the case of SLNs, an increase of the sonication time in the protocol used in this project could help to produce smaller SLNs. Moreover, different lipids and surfactant should be investigated to obtain particles with the desired properties.

Further optimization of the NPs must be performed in order to increase the therapeutic potential of the drugs. For instance, different production techniques and materials can be employed. For what it concerns the double emulsion PLGA NPs, new protocols can be tested. For example, a first emulsion can be prepared adding Pluronic F-68 to the

organic phase consisting of PLGA in ethyl acetate and, to obtain the second emulsion, use double distilled water containing calcium chloride, as described by E. Cohen-Sela et al. [84]. This could help in order to try to obtain a higher EE for TC and, eventually, for the real drugs to encapsulate in the future. Besides, the encapsulation of drugs to reduce systemic side effects and increase their bioavailability must be studied for the other types of NPs produced in this project. In addition, surface modifications with specific proteins or antibodies able to target the brain may improve targeting and accumulation of the NPs in the brain tissue as well as increase the drugs' bioavailability.

Appendices

Appendix A

BCA Protein Assay

The BCA Protein Assay Kit from Thermo Scientific (Waltham, Massachusetts, USA) is a simple and reliable protein quantification method that can be used to determine protein concentration in the range of 20-2000 μg/mL. The principle of this method is that proteins can reduce copper from Cu^{2+} to Cu^+ in an alkaline solution (i.e., the biuret reaction). This results in a purple color formation by bicinchoninic acid that strongly absorbs light at a wavelength of 562 nm. The amount of protein present in a solution is quantified by measuring the absorption spectra and comparing it with protein solutions with known concentrations.

The kit consists of two reagents to be used in a proportion 50:1 (Reagent A to Reagent B). Every well of the plate used for the measurement of the absorbance is prepared using 240 μL of a mix of the two reagents and 30 μL of the solution of interest.

Appendix B

Calibration Curve

To produce a linear calibration curve of TC dissolved in water, solutions of TC in water were prepared at a concentration of 0.00, 0.10, 0.20, 0.40, 0.60, 0.80 and 1.00 mg/mL. Every well of the plate was prepared by mixing 240 µL of the BCA kit solution and 30 µL of TC in water at different concentrations.

The calibration curve in Figure B.1 was obtained from the data in Table B.1. The procedure to get this calibration curve, which was obtained as the average of a triplicate, is the following. Firstly, the samples are prepared, and their absorbance is measured at a wavelength of 562 nm using a Synergy 2 Microplate Reader (BioTek, UK). The absorbance measurement is taken after 30 minutes of incubation at 37°C. Therefore, after the data were collected, the average absorbance corresponding to every concentration was calculated. Lastly, the average blank (i.e., the absorbance obtained for a concentration of 0.0 mg/mL) was subtracted from the average absorbance obtained for every concentration.

	Concentration [mg/mL]						
	0.00	0.10	0.20	0.40	0.60	0.80	1.00
Absorbance 1	0.107	0.21	0.271	0.381	0.469	0.568	0.655
Absorbance 2	0.120	0.221	0.278	0.381	0.457	0.523	0.622
Absorbance 3	0.108	0.215	0.294	0.415	0.551	0.659	0.779
Average absorbance	0.112±0.006	0.215±0.004	0.281±0.009	0.392±0.016	0.4492±0.042	0.5583±0.057	0.685±0.068
Absorbance without blank	0.000±0.007	0.104±0.006	0.169±0.012	0.281±0.019	0.381±0.051	0.472±0.069	0.574±0.083

Table B.1: Absorbance data used to compute the example calibration curve

Figure B.1 shows the calibration curve, where the y-axis corresponds to the absorbance value and the x-axis to the concentration of the compound in mg/mL. Every point is expressed as mean ± SD.

The Kit happened to return a slightly different result every time it is used, so it was necessary to prepare a calibration curve every time the Kit had to be used.
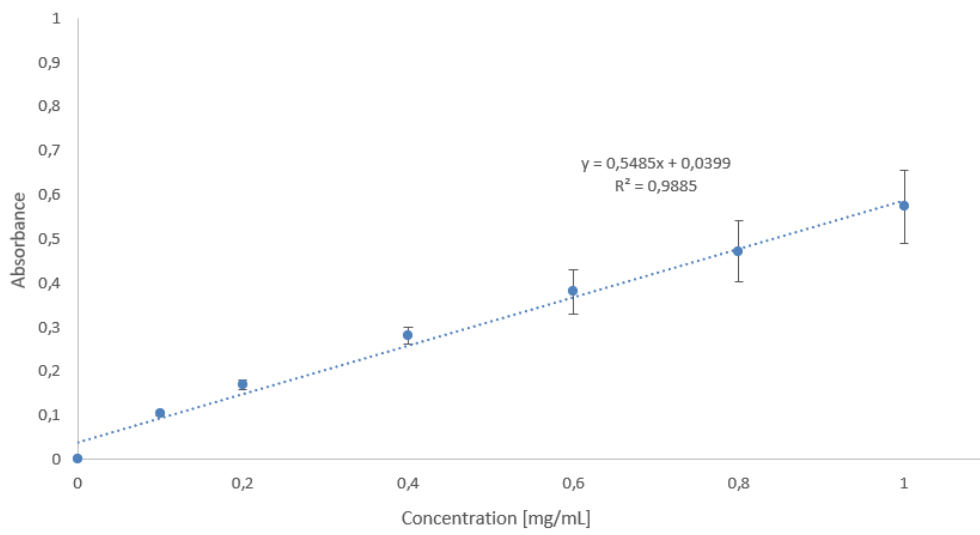
Figure B.1: Example of calibration curve of TC in water

Appendix C

Entrapment Efficiency

In this Appendix, an example of the calculation of the EE is given. The EE is measured using an indirect method, which consists in the measurement of the drug outside of the nanoparticles. To quantify the EE, the supernatant and the NPs are separated for every time point. The absorbance of the supernatant is then measured using the BCA Protein Assay Kit, which returns the maximum absorbance at a wavelength of 562 nm. The calculation of the EE was performed using the following data:

$$
\begin{aligned}
Total\ amount\ of\ drug\ &=\ 3.34\ mg \\
Drug\ concentration\ &=\ \frac{Total\ amount\ drug}{Volume} = \frac{3.34}{3}\ = 1.11\ mg/mL \\
Calibration\ curve\ equation:\ y\ &=\ 0.5485x + 0.0402 \\
Absorbance_{LOADED}\ &=\ 0.547 \\
Absorbance_{BLANK}\ &=\ 0.150
\end{aligned}
\tag{C.1}
$$

Firstly, the difference between the absorbance of the sample containing the drug and the one not containing (control) it is calculated. This allows to obtain the absorbance due to the compound only. Indeed, the absorbance caused by the free PLGA and PVA is supposed to be the same in both the loaded and the non-loaded NPs. In the case of the example, this lead to:

$$
\begin{aligned}
Absorbance_{DRUG}\ &=\ Absorbance_{LOADED}\ -\ Absorbance_{BLANK}\ = \\
&=\ 0.547 - 0.150\ =\ 0.397
\end{aligned}
\tag{C.2}
$$

The concentration of the drug corresponding to the absorbance is then calculated using the CC:

$$
Drug\ concentration\ [mg/mL]\ =\ \frac{0.3970 - 0.0402}{0.5485} = 0.6505\ mg/mL
\tag{C.3}
$$

Finally, the EE is computed:

$$EE(\%) = \frac{total\ amount\ of\ drug - amount\ of\ free\ drug}{total\ amount\ of\ drug} \times 100 =$$
$$= \frac{1.11 - 0.65}{1.11} \times 100 = 41.44\% \tag{C.4}$$

References

[1] Mucke L. Alzheimer's disease. Nature. 2009 Oct 15. 461:895–897

[2] Lane CA, Hardyb J, Schott JM. Alzheimer's disease. European Journal of Neurology. 2018. 25:59–70

[3] Ballard C, Gauthier S, Corbett A, Brayne C, Aarsland C, Jones E. Alzheimer's disease. Lancet. 2011 Mar 2. 377:1019–1031

[4] Blennow K, De Leon MJ, Zetterberg H. Alzheimer's disease. Lancet. 2006; 368:387–403

[5] Hardy JA, Higgins GA. Alzheimer's Disease: The Amyloid Cascade Hypothesis. Science. 1992 Apr 10. 184-185

[6] Barage SH, Sonawane KD. Amyloid cascade hypothesis: Pathogenesis and therapeutic strategies in Alzheimer's disease. Neuropeptides. 2015 Jul 2. 52:1-18

[7] Karran E, Mercken M, De Strooper B. The amyloid cascade hypothesis for Alzheimer's disease: an appraisal for the development of therapeutics". Nature Reviews. 2011 Sep. 10:698-712

[8] Meraz-Rios MA, Lira-De León KI, Campos-Peña V, De Anda-Hernández MA, Mena-López R. Tau oligomers and aggregation in Alzheimer's disease. Journal of Neurochemistry. 2010. 112:1353-1367

[9] Liu D, Yang F, Xiong F, Gu N. The Smart Drug Delivery System and Its Clinical Potential. Theranostics. 2016 Jun 7. 6(9):1306-1323

[10] Fish PV, Steadmana D, Baylea D, Whiting P. New approaches for the treatment of Alzheimer's disease. Bioorganic & Medicinal Chemistry Letters. 2019 Nov 19. 29:125-133

[11] Vaz M, Silvestre S. Alzheimer's disease: Recent treatment strategies. European Journal of Pharmacology. 2020 Sep 15

[12] Klafki HW, Staufenbiel M, Kornhuber J, Wiltfang J. Therapeutic approaches to Alzheimer's disease. Brain. 2006 Oct 3. 129:2840–2855

[13] Thorsett ED and Latimer LH. Therapeutic approaches to Alzheimer's disease. Current Opinion in Chemical Biology. 2000. 4:377–382

[14] Sun X, Jin L, Ling P. Review of drugs for Alzheimer's disease. Drug Discoveries & Therapeutics. 2012. 6(6):285-290

[15] Cummings J. Lessons Learned from Alzheimer Disease: Clinical Trials with Negative Outcomes. Clinical and Translational Science. 2018 Aug 2. 11:147–152

[16] Metha D, Jackson R, Paul G, Shi J, Sabbagh M. Why do trials for Alzheimer's disease drugs keep failing? A discontinued drug perspective for 2010–2015. Expert Opinion on Investigational Drugs. 2017 Jun. 26:735–739

[17] Casey DA, Antimisiaris D, O'Brien J. Drugs for Alzheimer's Disease: Are They Effective?". Pharmacy & Therapeutics. 2010 Jan 21. 35:208–211

[18] Bartus R. The cholinergic hypothesis of geriatric memory dysfunction. Science. 1982. 217:408–414

[19] Ferreira-Vieira TH, Guimaraes IM, Silva FR, Ribeiro FM. Alzheimer's Disease: Targeting the Cholinergic System. Current Neuropharmacology. 2016. 14:101-115

[20] Suzuki K, Iwate A, Iwatsubo T. The past, present, and future of disease-modifying therapies for Alzheimer's disease. Proceedings of the Japan Academy. 2017. 93:757–771

[21] Salomone S, Caraci F, Leggio GM, Fedotova J, Drago F. New pharmacological strategies for treatment of Alzheimer's disease: focus on disease modifying drugs. British Journal of Clinical Pharmacology. 2011 Apr 11. 73:504–517

[22] Yiannopoulou KG, Anastasiou AI, Zachariou V, Pelidou SH. Reasons for Failed Trials of Disease-Modifying Treatments for Alzheimer Disease and Their Contribution in Recent Research. Biomedicines. 2019 Dec 9. 9:97-113

[23] Ghezzi L, Scarpini E, Galimberti D. Disease-modifying drugs in Alzheimer's disease. Drug Design, Development and Therapy. 2013 Oct 3. 7:1471–1479

[24] Lemere CA. Immunotherapy for Alzheimer's disease: hoops and hurdles. Molecular Neurodegeneration. 2013. 8:36-42

[25] Valiukas Z, Ephraim R, Tangalakis K, Davidson M, Apostolopoulos V. Immunotherapies for Alzheimer's Disease—A Review. Vaccines. 2022 Sep 14. 10:1527-1544

[26] Walsh S, Merrick R, Milne R, Brayne C. Aducanumab for Alzheimer's disease? Patients and families need hope, not false hope. British Medical Journal. 2021 Jul 5. 374:1682-1683

[27] Beshir SA, Aadithsoorya AM, Parveen A, Hussain N. Aducanumab Therapy to Treat Alzheimer's Disease: A Narrative Review. International Journal of Alzheimer's Disease. 2022 Mar 9.

[28] Vaz M, Silva V, Monteiro C. Role of Aducanumab in the Treatment of Alzheimer's Disease: Challenges and Opportunities. Clinical Interventions in Aging. 2022 Sep 17. 17:797-810

[29] Hoy SM. Lecanemab: First Approval. Drugs. 2023 Mar 1. 83:359–365

[30] Walsh S, Merrick R, Richard E. Lecanemab for Alzheimer's disease. New trial reports little to celebrate for patients and carers. British Medical Journal. 2022 Dec 19. 1682:374-375

[31] Pandit R, Chen L, Gotz J. The blood-brain barrier: Physiology and strategies for drug delivery. Advanced Drug Delivery Reviews. 2020 Nov 29. 165-166:1-14

[32] Keaney J and Campbell M. The dynamic blood–brain barrier. The FEBS Journal. 2015 Aug 12. 282:4067-4079

[33] Wong AD, Ye M, Levy AF. The blood–brain barrier: an engineering perspective. Frontiers in Neuroengineering. 2013 Aug. 6:1-22

[34] Abbott NJ, Patabendige AAK, Dolman DEM. Structure and function of the blood–brain barrier. Neurobiology of Disease. 2010 Aug 5. 37:13–25

[35] Gosselet F, Loiola RA, Roig A. Central nervous system delivery of molecules across the blood-brain barrier. Neurochemistry International. 2021 Jan 2. 14:2719-2757

[36] Banks WA. Characteristics of compounds that cross the blood-brain barrier. BMC Neurology. 2009 Feb 2. 9:1-5

[37] Turner PV, Brabb T, Pekow C. Administration of Substances to Laboratory Animals: Routes of Administration and Factors to Consider. Journal of the American Association for Laboratory Animal Science. 2011 Sep. 50:600–613

[38] Lalatsa A, Schatzlein AG, Uchegbu IF. Strategies To Deliver Peptide Drugs to the Brain. Molecular Pharmaceutics. 2014 Mar 6. 11:1081-1093

[39] Frokjaer S and Otzen DE. Protein drug stability: a formulation challenge. Nature Reviews. 2005 Apr. 4:298-306

[40] Griffin BT, Guo J, Presas E. Pharmacokinetic, pharmacodynamic and biodistribution following oral administration of nanocarriers containing peptide and protein drugs. Advanced Drug Delivery Reviews. 2016 Jun 16. 106:367-380

[41] Vohra M, Amir M, Sharmaa S. Formulation strategies for nose-to-brain drug delivery in Alzheimer's disease. Health Science Review. 2023 Jan 3. 6:1-8

[42] Erdo F, Borsa LA, Farkasa D. Evaluation of intranasal delivery route of drug administration for brain targeting. Brain Research Bulletin. 2018 Oct 23. 143:155-170

[43] Cunha S. Improving Drug Delivery for Alzheimer's Disease Through Nose-to-Brain Delivery Using Nanoemulsions, Nanostructured Lipid Carriers (NLC) and in situ Hydrogels. International Journal of Nanomedicine. 2021. 16:4373-4390

[44] Patel MM and Patel BM. Crossing the Blood–Brain Barrier: Recent Advances in Drug Delivery to the Brain. CNS Drugs. 2017 Jan 18. 31:109–133

[45] Liu J. The shape of things to come: importance of design in nanotechnology for drug delivery. Therapeutic Delivery. 2012 Feb. 3:181-194

[46] Alam MI, Bega S, Samadb A. Strategy for effective brain drug delivery. European Journal of Pharmaceutical Sciences. 2010. 40:385-403

[47] Lee BK, Yun JH, Park K. Smart nanoparticles for drug delivery: Boundaries and opportunities. Chemical Engineering Science. 2015 July 1. 125:158-164

[48] Partridge WM. Blood–brain barrier delivery. Drug Discovery Today. 2007 Jan. 30:235–258

[49] Pardridge W. Blood-Brain Barrier Drug Targeting: The Future of Brain Drug Development. Molecular Interventions. 2003 Mar. 3:90-105

[50] De Jong WH and Borm PJA. Drug delivery and nanoparticles: Applications and hazards. International Journal of Nanomedicine. 2022 Oct 9. 3:133–149

[51] Mirakabad FST, Nejati-Koshki K, Akbarzadeh2 A, Yamchi5 MR. PLGA-Based Nanoparticles as Cancer Drug Delivery Systems. Asian Pacific Journal of Cancer Prevention. 2014. 15:517-535

[52] Acharya S and Sahoo SK. PLGA nanoparticles containing various anticancer agents and tumour delivery by EPR effect. Advanced Drug Delivery Reviews. 2011 Oct 20. 63:170-183

[53] Del Amo L. Surface Functionalization of PLGA Nanoparticles to Increase Transport across the BBB for Alzheimer's Disease. Applied sciences. 2021. 11:4305

[54] Makadia HK and Siegel SJ. Poly Lactic-co-Glycolic Acid (PLGA) as Biodegradable Controlled Drug Delivery Carrier. Polymers. 2011 Aug 26. 3:1377-1397

[55] Feczkó T, Toth J, Dosa GY. Optimization of protein encapsulation in PLGA nanoparticles. Chemical Engineering and Processing: Process Intensification. 2011. 50:757-765

[56] Aderibigbe BA and Naki T. Chitosan-Based Nanocarriers for Nose to Brain Delivery. Applied Sciences. 2019 May 30. 9:2219

[57] Yu S, Xua X, Fengc J, Liub M. Chitosan and chitosan coating nanoparticles for the treatment of brain disease. International Journal of Pharmaceutics. 2019 Feb 14. 560:282-293

[58] Rassu G, Soddu E, Cossu M, Gavini E. Particulate formulations based on chitosan for nose-to-brain delivery of drugs. A review. Journal of Drug Delivery Science and Technology. 2015 May 4. 21:5016

[59] Garud A, Singh D, Garud N. Solid Lipid Nanoparticles (SLN): Method, Characterization and Applications. International Current Pharmaceutical Journal. 2012. 1(11):384-393

[60] Khatak S. Solid lipid nanoparticles - A review. International Journal of Applied Pharmaceutics. 2013 Feb 5. 5:8-18

[61] Mehnert W and Mäder K. Solid lipid nanoparticles: Production, characterization and applications. Advanced drug delivery reviews. 2012. 47:165-196

[62] Mukherjee S, Ray S, Thakur RS. Solid Lipid Nanoparticles: A Modern Formulation Approach in Drug Delivery System. Indian Journal of Pharmaceutical Sciences. 2009 Aug. 71:349-358

[63] Almeida AJ and Souto E. Solid lipid nanoparticles as a drug delivery system for peptides and proteins. Advanced Drug Delivery Reviews. 2007 May 1. 59:478–490

[64] Cohen-Sela E, Teitlboim S, Chorny M, Koroukhov N. Single and Double Emulsion Manufacturing Techniques of an Amphiphilic Drug in PLGA Nanoparticles: Formulations of Mithramycin and Bioactivity. Journal of Pharmaceutical Sciences. 2009 Jul 8. 98:1452-1462

[65] Iqbal M, Zafar N, Fessi H, Elaissari A. Double emulsion solvent evaporation techniques used for drug encapsulation". International Journal of Pharmaceutics. 2015 Oct 29. 496:173-190

[66] Tu F and Lee D. Controlling the Stability and Size of Double-Emulsion-Templated Poly(lactic-co-glycolic) Acid Microcapsules. Langmuir. 2012 Jun 5. 28:9944-9952

[67] Madej M, Kurowska N, Strzalka-Mrozik B. Polymeric Nanoparticles—Tools in a Drug Delivery System in Selected Cancer Therapies. Applied Sciences. 2022 Sep 21. 12:9479

[68] Zielinska A, Carreiró F, Oliveira AM, Neves A, Pires B. Polymeric Nanoparticles: Production, Characterization, Toxicology and Ecotoxicology. Molecules. 2020 Aug 15. 25:3731

[69] Karam M, Fahs D, Maatouk B, Safi B, Jaffa AA, Mhanna R. Polymeric nanoparticles in the diagnosis and treatment of myocardial infarction: Challenges and future prospects. Materials Today Bio. 2020 Apr 4. 14:1-30

[70] Kaszuba M, McKnight D, Connah MT, McNeil-Watson FK, Nobbmann U. Measuring sub manometer sizes using dynamic light scattering. Journal of Nanoparticle Research. 2008 Oct 26. 10:823–829

[71] Falke S and Betzel C. Dynamic Light Scattering (DLS). Springer International Publishing. 2019. 173-193

[72] Stetefeld J, McKenna SA, Patel TR. Dynamic light scattering: a practical guide and applications in biomedical sciences. Biophysical Reviews. 2016 Oct 6. 8:409–427

[73] Lorber B, Fischer F, Bailly M, Roy H, Kern D. Protein Analysis by Dynamic Light Scattering: Methods and Techniques for Students. Biochemistry and molecular biology education. 2012 Jul 23. 40:372–382

[74] Lim J, Yeap1 SP, Che1 HX, Low1 SC. Characterization of magnetic nanoparticle by dynamic light scattering. Nanoscale Research Letters. 2013. 8:381-395

[75] Pecora R. Dynamic light scattering measurement of nanometer particles in liquids. Journal of Nanoparticle Research. 2020 June 14. 2:123–131

[76] Bhattacharjee S. DLS and zeta potential – What they are and what they are not?. Journal of Controlled Release. 2016 Jun 10. 235:337-351

[77] Lorin M, Miller WG. Spectrophotometry. Contemporary Practice in Clinical Chemistry. 2020. 4:119-133

[78] Duong VA, Nguyen TTL, Maeng HJ. Preparation of Solid Lipid Nanoparticles and Nanostructured Lipid Carriers for Drug Delivery and the Effects of Preparation Parameters of Solvent Injection Method. Molecules. 2020 Oct 18. 25:4781

[79] Saha D, Kumar S, Ray D, Mata J, Aswal VK. Structure and stability of biodegradable polymer nanoparticles in electrolyte solution. Materials Letters: X. 2021 Jun. 10:1-4

[80] Chiu HI, Samad NA, Fang L, Lim V. Cytotoxicity of targeted PLGA nanoparticles: a systematic review. Royal Society Of Chemistry. 2021 Mar 1. 11(16):9433-9449

[81] Sahoo SK, Panyam J, Prabha S, Labhasetwar V. Residual polyvinyl alcohol associated with poly (D,L-lactide-co-glycolide) nanoparticles affects their physical properties and cellular uptake. Journal of Controlled Release. 2002 Jul 18. 82:105-114

[82] Rampino A, Borgogna M, Blasi P, Bellich B, Cesaro A. Chitosan nanoparticles: Preparation, size evolution and stability. International Journal of Pharmaceutics. 2013 Oct 15. 455: 219-228

[83] Kaur S, Manhas P, Swami A. Bioengineered PLGA-chitosan nanoparticles for brain targeted intranasal delivery of antiepileptic TRH analogues. Chemical Engineering Journal. 2018 Aug 15. 346: 630-639

[84] Cohen-Sela E, Chorny M, Koroukhov N. A new double emulsion solvent diffusion technique for encapsulating hydrophilic molecules in PLGA nanoparticles. Journal of Controlled Release, 2009 Jan 19. 133(2): 90–95

[85] Cruz KP, Patricio BFC, Pires VC. Development and Characterization of PLGA Nanoparticles Containing 17-DMAG, an Hsp90 Inhibitor. Frontiers in Chemistry, 2021 May 13. 9:644927

[86] Barichello JM, Morishita M, Takayama K, Nagai T. Encapsulation of Hydrophilic and Lipophilic Drugs in PLGA Nanoparticles by the Nanoprecipitation Method. Drug Development and Industrial Pharmacy. 1999 Apr. 25(4):471-476

[87] Scherließ R and Janke J. Preparation of Poly-Lactic-Co-Glycolic Acid Nanoparticles in a Dry Powder Formulation for Pulmonary Antigen Delivery. Pharmaceutics. 2021 Aug 3. 13(8): 1196

[88] Panigrahi D, Sahu PK, Swain S, Verma RK. Quality by design prospects of pharmaceuticals application of double emulsion method for PLGA loaded nanoparticles. SN Applied Sciences. 2021. 3:638

[89] Haggag YA, Abosalha AK, Tambuwala M. Polymeric nanoencapsulation of zaleplon into PLGA nanoparticles for enhanced pharmacokinetics and pharmacological activity. Biopharmaceutics & Drug Disposition. 2020 Dec 15. 42(1):12–23

[90] Madani F, Esnaashari SS, Mujokoro B. Investigation of Effective Parameters on Size of Paclitaxel Loaded PLGA Nanoparticles. Advanced Pharmaceutical Bulletin. 2018 Mar. 8(1): 77-84

[91] Alkholief M, Kalam MA, Khalid Anwer MD, Alshamsan AWS. Effect of Solvents, Stabilizers and the Concentration of Stabilizers on the Physical Properties of Poly(D,L-lactide-co-glycolide) Nanoparticles: Encapsulation,In Vitro Release of Indomethacin and Cytotoxicity against HepG2-Cell. Pharmaceutics. 2022 Apr 15. 14(4):870

[92] Musyanovych A, Schmitz-Wienke J, Mailänder V, Walther P, Landfester K. Preparation of Biodegradable Polymer Nanoparticles by Miniemulsion Technique and Their Cell Interactions. Macromolecular Bioscience. 2008 Feb 11. 8(2): 127–139

[93] Lu B, Lv X, Le Y. Chitosan-Modified PLGA Nanoparticles for Control-Released Drug Delivery. Polymers. 2019 Feb. 11(2):304

[94] Wang Y, Li P, Kong L. Chitosan-Modified PLGA Nanoparticles with Versatile Surface for Improved Drug Deliver. AAPS PharmSciTech. 2013 Jun. 14:585–592

[95] Ways TMM, Lau WM, Khutoryanskiy VV. Chitosan and Its Derivatives for Application in Mucoadhesive Drug Delivery Systems. 2018 Mar. 10(3):267

[96] Popescu R, Ghica MV, Dinu-Pîrvu CE, Anuța V, Lupuliasa D, Popa L. New Opportunity to Formulate Intranasal Vaccines and Drug Delivery Systems Based on Chitosan. International Journal of Molecular Sciences Review, 2020 Jul 16. 21:5016

[97] Righeschi C, Bergonzi MC, Isacchi B, Bazzicalupi c, Gratteri P, Bilia AL. Enhanced curcumin permeability by SLN formulation: The PAMPA approach.LWT - Food Science and Technology. 2016 Mar. 66:475-483

[98] Freitas C and Muller RH. Effect of light and temperature on zeta potential and physical stability in solid lipid nanoparticle (SLN) dispersions. International Journal of Pharmaceutics. 1998 Jun 15. 168(2):221–229

[99] Morsi NM, Ghorab DN, Badie HA. Brain targeted solid lipid nanoparticles for brain ischemia: preparation and in vitro characterization, Pharmaceutical Development and Technology. 2013 May-Jun. 18(3):736-744

[100] Kalaycioglu GD and Aydogan N. Preparation and investigation of solid lipid nanoparticles for drug delivery. Colloids and Surfaces A: Physicochemical and Engineering Aspects. 2016 Dec 5. 510:77-86